SHAPE OPTIMIZATION OF HELICOPTER SUBFLOOR INTERSECTION ELEMENT UNDER CRASH LOADING

A THESIS SUBMITTED TO
THE GRADUATE SCHOOL OF NATURAL AND APPLIED SCIENCES
OF
MIDDLE EAST TECHNICAL UNIVERSITY

BY

MUSTAFA OKAN TÜRE

IN PARTIAL FULFILLMENT OF THE REQUIREMENTS
FOR
THE DEGREE OF MASTER OF SCIENCE
IN
MECHANICAL ENGINEERING

SEPTEMBER 2017

Approval of the thesis:

SHAPE OPTIMIZATION OF HELICOPTER SUBFLOOR INTERSECTION ELEMENT UNDER CRASH LOADING

submitted by **MUSTAFA OKAN TÜRE** in partial fulfillment of the requirements for the degree of **Master of Science in Mechanical Engineering Department, Middle East Technical University** by,

Prof. Dr. Gülbin Dural Ünver
Dean, Graduate School of **Natural and Applied Sciences** _____

Prof. Dr. Tuna Balkan
Head of Department, **Mechanical Engineering** _____

Prof. Dr. Serkan Dağ
Supervisor, **Mechanical Engineering Department, METU** _____

Examining Committee Members:

Assist. Prof. Dr. Gökhan O. Özgen
Mechanical Engineering Department, METU _____

Prof. Dr. Serkan Dağ
Mechanical Engineering Department, METU _____

Prof. Dr. Hakan I. Tarman
Mechanical Engineering Department, METU _____

Assist. Prof. Dr. Hüsnü Dal
Mechanical Engineering Department, METU _____

Assist. Prof. Dr. Barış Sabuncuoğlu
Mechanical Engineering Department, UTAA _____

Date: **15.09.2017**

I hereby declare that all information in this document has been obtained and presented in accordance with academic rules and ethical conduct. I also declare that, as required by these rules and conduct, I have fully cited and referenced all material and results that are not original to this work.

Name, Last Name: MUSTAFA OKAN TÜRE

Signature :

ABSTRACT

SHAPE OPTIMIZATION OF HELICOPTER SUBFLOOR INTERSECTION ELEMENT UNDER CRASH LOADING

TÜRE, Mustafa Okan
M.S., Department of Mechanical Engineering
Supervisor : Prof. Dr. Serkan Dağ

September 2017, 107 pages

The aim of the crashworthiness is maintaining a survivable space for occupants and absorb crash energy as much as possible. The statistics showed that 85% of all rotorcraft accidents can be survivable[1]. Thus, crashworthy design has direct effect on occupants' survival. This thesis analyses a longitudinal beam and lateral frame intersection point structure on helicopter subfloor. Analysis is performed on ABAQUS Dynamic/Explicit solver. Analysis includes high deformation levels, self-contact and nonlinearities are included. 110 kg mass is dropped on test structure to simulate crush. The test specimen impacted at 7 m/s vertical speed. To improve the design concept, energy absorption capability of the structure will be examine. Test verification is performed in the first part. After modelling techniques set with verification, geometric optimization is performed to get better energy absorbing capability of subfloor structure. Genetic algorithm is used while finding the best crashworthy solution in our design limits. At the first part of optimization only geometric variables are investigated. At the second part, material is added as another parameter. Optimum energy absorber structure is aimed as a result of this process.

Keywords: Crash, Helicopter, Subfloor structure, Energy absorption, Geometric optimization

ÖZ

ÇARPMA KOŞULU ALTINDA HELİKOPTER ZEMİN BİRLEŞME NOKTALARININ ŞEKİL OPTİMİZASYONU

TÜRE, Mustafa Okan
Yüksek Lisans, Makine Mühendisliği Bölümü
Tez Yöneticisi : Prof. Dr. Serkan Dağ

Eylül 2017 , 107 sayfa

Bu tezin amacı helikopter yapısının boyutlarını optimize ederek, yapının enerji emilimini maksimize hale getirmektir.Araştırmalara göre, gereken önlemler alındığı takdirde, helikopter kazalarının %85'inde ölümler engellenebilir[1]. Özetle, kaza dayanımı yolcular için hayati öneme sahiptir. Bu tezde helikopterin zemininde bulunan kiriş ve çerçevelerin birleşim noktalarının şekilleri optimize edilecektir. Çarpışma simülasyonu ABAQUS sonlu elemanlar programında yapılmıştır. Çarpışmadan dolayı simülasyon yüksek miktarda temas ve doğrusalsızlık içermektedir. 110 kilogram yük test modeline 7 m/s hızla dik olarak çarpmaktadır. Modelin tasarımını geliştirmek için enerji emiş kapasitesi incelenmiştir. Tezin ilk bölümünde referans makaleden alınan test sonuçları doğrulanmıştır. İkinci kısımda modelin geometrik olarak optimizasyonu yapılmıştır. Optimizasyon kısmında genetik algoritma kullanılmıştır. Optimizasyonun ilk kısmında tek bir malzeme ile parçaların boyutları belirlenirken, ikinci kısımda malzeme de parametre olarak optimizasyona dahil edilmiştir. Bu yolla modelin en iyi şekilde enerji tasarımına ulaşılmaya çalışılmıştır.

Anahtar Kelimeler: Çarpışma, Helikopter, Helikopter zemin yapısı, Enerji emiş miktarı, Geometrik optimizasyon

To my family and my cousin Ahmet Emre ÜSTÜNGEL

ACKNOWLEDGMENTS

This thesis was conducted under the supervision of Prof. Dr. Serkan Dağ. I would like to express my sincere appreciation for the support, encouragement, guidance and insight he has provided throughout the thesis.

TABLE OF CONTENTS

LIST OF TABLES

TABLES

LIST OF FIGURES

FIGURES

LIST OF ABBREVIATIONS

EASA	European Aviation Safety Agency
FE	Finite Element
FEM	Finite Element Method
DEA	Deployable Energy Absorber
GA	Genetic Algorithm
RF	Reaction Force

LIST OF SYMBOLS

E	Modulus of Elasticity
K_0	Linear Matrix of the System
K_σ	Initial Stress Matrix
K_u	Initial Displacement Matrix
$\lambda_c r$	Critical Loading Multiplier
v	Respective Post Buckling Form
L	Column Length
K	Effective Length Comes from Boundary Conditions
$\frac{KL}{r}$	Slenderness Ratio of the Column
σ_t	Tangent Modulus Stress
c	Flange Length
t	Flange Thickness
F_{av}	Average Crushing Force
δ	Effective Crushing Distance Factor
σ_o	Characteristic Flow Stress
σ_y	Material Yield Stress
W_C	Total Absorbed Energy
H	Flange Width
T	Flange Thickness
F	Force Vector
S	Position Vector
C	Path Integration
p	Material Strain Rate Parameter 1
D	Material Strain Rate Parameter 2
$\dot{\epsilon}$	Strain Rate
$\sigma(\epsilon, \dot{\epsilon})$	Cowper-Symonds Stress

CHAPTER 1

INTRODUCTION

Researches have revealed that many helicopter crashes are survivable, if certain precautions are taken. Crash has effects on occupant both at instant crash event and post-crash dangers. Post-crash dangers like fire, jammed exists and drowning[1]. These dangers are prevented by implementing several systems to the helicopter. At instant of a crash event, high load is created and transmitted through subfloor structure to occupants. These high loads can often cause fatal injuries. Crash deformation is mostly conclude as structural framework collapse rather than leading efficient energy dissipation[2]. Load can be reduced by changing design or implementing crash absorber systems to the helicopter. Structures and connections are redesigned to get crashworthy helicopter. When helicopter crashes are analyzed, vertical crashes are observed to have the majority. In these kind of crashes, high loads are transmitted to the occupants[3]. These loads are transmitted through the landing gear, fuselage and seats. In addition to direct load injuries, occupants also suffer from cabin collapse. After crash, survivable space should remain inside the cabin. High mass items like transmission and engine should also be prevented from collapsing into the cabin.

In many crashes, emergency landing occurs with retracted landing gears[3]. Thus, importance of the subfloor structure has increased. In crash, large deformations occur on the helicopter structure. To achieve efficient energy absorption, progressive crush is needed rather than structural framework collapse[4] [5]. If the structures cannot achieve the energy-absorbing work well, the remaining energy is absorbed by the occupants causing fatal injuries. For this reason, energy absorbing design is needed at the subfloor structure to minimize the occupants' injuries. Load passes from floor first before transmitted to the occupants. That's why energy absorbing capacity of the floor structure should be increased as much as possible.

1.1 Thesis Objective

The objective of this thesis is to find optimum shape, thickness and material for sub-floor intersection element of the helicopter. In the first part of the thesis, test results are verified. The modelling methodology of the test is learned. In the second part, a parametric code is generated and several different models are investigated. The results of these models results are compared in accordance with genetic algorithm optimization method. The best design is determined in our design space by comparing their force-shortening diagrams, energy absorbing capacities and crushing forces. In second part, another parameter added to optimization, that is material. The main aim is to find the best section size and material to increase the crashworthiness.

1.2 Crashworthiness

In 1960s, the US army started to investigate past crashes. When past helicopter crashes were investigated, it was found that large numbers of crashes had been survivable. The importance of the crashworthiness has increased from that point. After that, many standards have been established[8]. These standards are established to provide minimum requirement of crashworthy structure. The latest helicopters are designed to maintain enough space to occupant after crash. Another important necessity is to decrease high deceleration at the peak loads. Structure should minimize weight and cost, maintain cabin floor structural integrity and resist static loads while providing high energy absorption capacity. Engineers are aiming to find better ways to provide an envelope of survivability. Kindervater et al. argues on the requirements to improve the energy absorption capacity such as,

- Uncritical distribution of ground reaction and seat load
- Eliminate high peak loads with controlled load concept
- Satisfy cabin structural wholeness
- Minimize cost and penalties[9]

As it can be seen from Figure 2.1 - Helicopter Energy Absorbers, three different energy absorbers exist below occupants. Seat, cabin structure, floor and landing gear can be coupled to help minimize crash effects. If you come to think about crash with

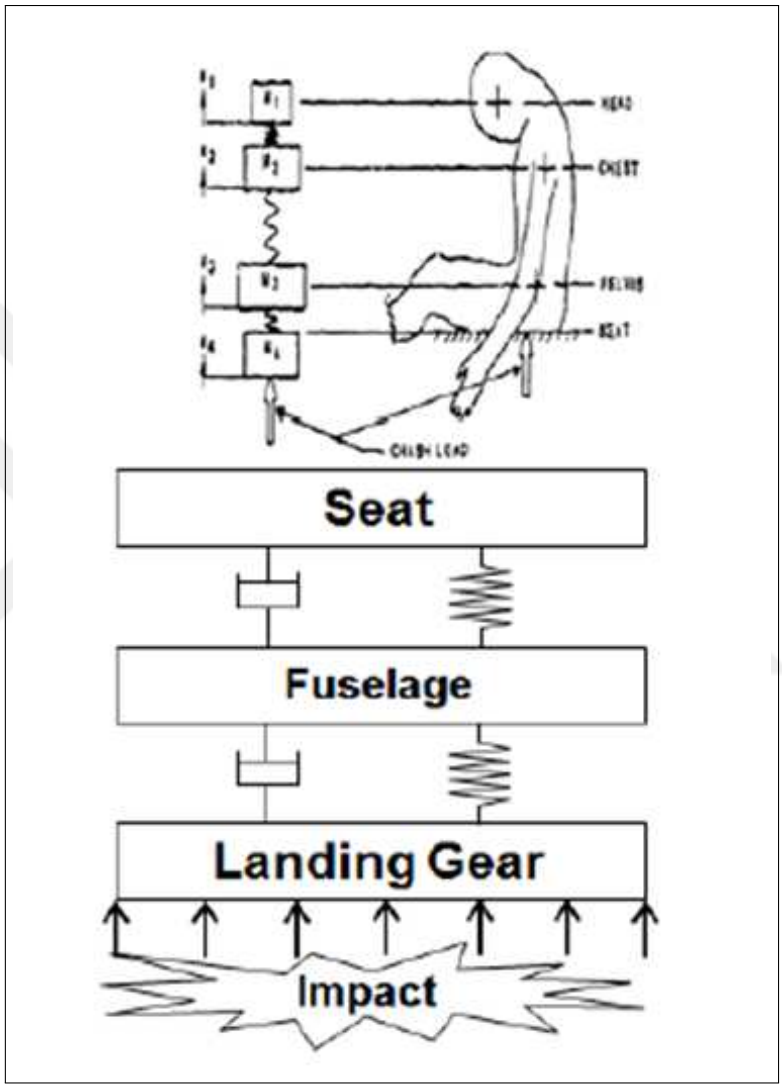

Figure 1.1: Helicopter Energy Absorbers

retracted landing gear, fuselage, seat and occupants should absorb the whole energy. The question is how to control the energy absorption characteristic of structure to deform in order to dissipate energy as much as possible. This absorption can be possible with planned bucking of the structure. If controlled crushing sequence is rightly set up, energy absorption takes place with plastic collapse. A structure, designed according to controlled crushing sequence is better energy absorber than the structure which is plastically deformed due to Euler buckling.

In subfloor structure, the most important part is floor intersection points. The energy absorbing characteristic of a subfloor structure depends on several factors including material type, geometry, rivet type and the overall topology of the framework. Of the interest in terms of energy absorption are the intersection joints of the beams and bulkheads. These intersections act like hard point stiff columns where high peak loads occur. The role of these intersections is fundamentally important and as such, it is essential that the structural elements at these intersections are studied and designed appropriately[10].

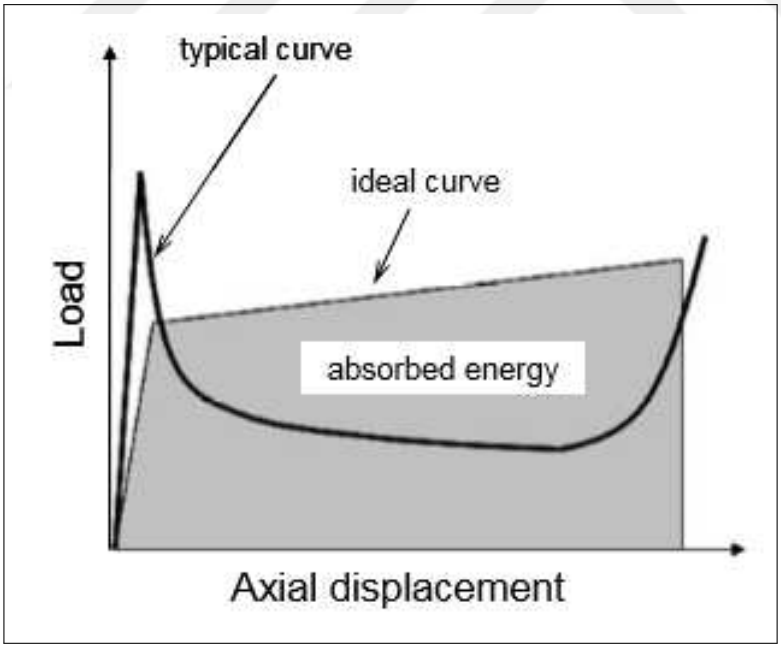

Figure 1.2: Ideal Load - Shortening Curve

For this reason, controlled collapse is very important to dissipate energy. In Figure 1.2 - Ideal Load - Shortening Curve, the wanted crash response has compared with

typical crash response. The stiffness of the structure should decrease at the early stage.

1.3 Summary of Thesis Plan

This thesis is presented through seven chapters. An introduction is presented in chapter 1. Introduction includes problem outline, thesis objective, crashworthiness. The theoretical background and literature review about ABAQUS finite element model, helicopter subfloor structure, material applications and test-analysis correlation. Main structure of the developed test model correlation is described in chapter 3 by presenting an algorithm chart and giving the details on each step. Finite element model is correlated with test result. Model information and correlation results are given in chapter 4. In chapter 5, maximum reaction force of the force-displacement curve is aimed to minimize without any displacement constraint. 5 variables of assembly is accepted as design variables. In addition of five parameters, material is added as sixth variable in chapter 6. Magnesium and titanium is assigned to parts other than aluminium. The design objective is the same with first part which is minimizing peak load. Finally, Chapter 7 is devoted to discussion, conclusion remarks and possible future work.

CHAPTER 2

LITERATURE REVIEW AND THEORETICAL BACKGROUND

Crash-worthiness is known as the ability of an aircraft and its internal systems to protect occupants from injury in the event of a crash. Shanahan states that there are three major injury sources. These are high acceleration changes, direct contact with high mass items and crash environment factors such as fire, smoke, water and chemicals[1]. Occupant's crash protection is a main concern from first flight. Many crash protection concepts are developed since first flight. Although most of the concepts are developed many years ago, implementations have been started recently[11]. The main reason is that crash protective concepts are not beneficial for performance, efficiency and cost[12]. Now, regulations have been tighter. Aircraft designers have to take into account occupant's protection. European Aviation Safety Agency has certification specification for each kind of aircraft. In this certification specifications, emergency landing conditions and required conditions are specified.

2.1 Crashworthiness of Helicopter Subfloor Structures

Crashworthy helicopters become more important because of regulations and competition with other helicopters in market. In crash landing, the first requirement is to create ability of an aeronautical structure to ensure a vital space for the occupants during an impact[13]. Limiting acceleration is also critical in crash. Guida et. al studied about allocation of impact kinetic energy rather than investigate structure deformation. According to this approach, designing energy flow path and correlation of it become more significant[14]. Lanzi et al. studied about optimization of energy absorbing subsystems. They specify that occupants' protection can be achieved in-

tegrating gears, subfloor and seats[3]. As a matter of fact, emergency landing could occur with retracted landing gears, on water or on particularly soft soils. Accordingly, helicopters cannot always rely on the contribution of the landing gears to absorb the whole impact energy and then the subfloor and seat absorption characteristic become of major concern in generic crash conditions[15]. Many studies have been performed through the years with comparison of experimental and numerical activities. Crashworthy design of rotorcraft requires a systems approach in which various subcomponents work together to absorb and dissipate the kinetic energy of impact[16]. According to Marco Anghileri research, the intersection between spars and frames gives the greatest contribution to the impact energy absorption during crash landing[12]. In intersection point, it can create high peak of deceleration at the floor of the cabin causing harm to the occupants.

2.2 Material Applications

In aircraft, metallic materials are generally used as primary structural elements. Material behaviour is studied by various researchers. Although fall height and impact velocities are not the same, material behaviors are similar. Kindervater et al. have studied about material model development. They concluded that all vertical components fail in buckling and skin plays no role in energy absorbing process[9]. Thus, it can be concluded that structures which are parallel to crash direction are design variables in impact scenarios. Bisagni found that rivets are also buckled under loading[10]. Guida et al. state that in conventional metallic materials, the plastic collapse of structures subjected to impact phenomena is very important[14]. The two most important forms of collapse, involved in energy dissipation during the impact are flexural and axial collapse. It can dissipate the kinetic energy with remarkable efficiency using the hinges in the joint areas. Fyllingen et al. have studied about that progressive buckling and transition from progressive buckling to global bending are observed throughout the loading[5]. The crushing behaviour changes dramatically with changing tube lengths. Material properties, specimen length, specimen shape, boundary conditions, shape and size of the impacting object and impact velocity affect the buckling mode of the specimen. The crushing behaviour at fixed end affects eccentricity which is the

reason of transition bending. If length is increased over a range, transition between modes is appears.

Engineers try to implement aircraft energy absorber material either metallic or composite. Karagiozova et al. have studied dynamic effects on buckling. Peak load; fold lengths, axial compression and energy absorption capacity are studied. To find material influence, two different materials are used which are steel and aluminium. Impact forces and striking masses are altered for different samples. Energy absorbing capacity is related with plastic energy crushing distance behavior. The amount of plastic stress and plastic strains determine final shape of specimen. Higher initial speeds are observed higher initial peak load[2] [18]. It is found that cylindrical tube is an efficient crash energy absorber. This is due to the cylindrical tube's inertial and strain rate. These variables have important role on impact energy process. Dong-Kuk Kim et al. studied dynamic crashing and impact energy of tubes. When compressive load is applied, the resistive force increases dramatically[19]. First buckling occurs at the maximum resistive point. At second plastic fold, force is concentrated on the other side of the specimen. Cracks at the edges increase the amount of energy which is absorbed during crash. Shape of the plastic folds affected the impact energy absorption excessively[20]. It is found that increasing strain rate also decrease uniformity. However, impact absorption capacity remains constant. Increasing thickness affects energy absorption capacity poorly. Higher thickness specimen increase overall bending and decrease plastic fold.

Composites are also used as primary structural materials in aerospace structures lately. The researches and crash tests related to composite materials are increasing. Composite vehicle crash resistance requires system design aspects. In helicopters this includes the airframe, the landing gear, seats and restraint systems. The behaviour of generic energy absorbing composite airframe components representative for helicopters were simulated under crash conditions. Then results were compared to structural response and failure modes of test results[21].

Kindervater et al. evaluate the crash behaviour of composite structures under low velocity impact loads. They conclude some requirements to maintain cabin floor integrity and crash resistant sub-floor structures[9]. Ground reaction and seat load

should be distributed uniformly. Limitation of the deceleration forces by structural deformation should be satisfied. Floor model should have moderate initial stiffness and then constant force level if possible. The simulations proved that the modelling of the orthotropic dynamic behavior of composites can be improved using enhanced material laws[22].

Composite material technologies are also in progress in aerospace technologies. Even their lightweight and strength, implementation these materials into structures are not easy because of their complex failure modes compared to metallic materials[23]. Metals absorb energy by plastic deformation and buckling however composites have different failure modes like delamination and fiber rupture. Although implementing composites as an energy absorber material into aircraft is complex and expensive; it has huge future in this field.

2.3 Test - Analysis Correlation

With developing computer aided analysis programs, the idea of simulating crash with finite element programs has arisen. However, this includes some uncertainty such as model validation procedures, uncertainty in the test data, probabilistic techniques for test-analysis correlation[24]. At NASA, Karen et al. studied about how they can increase the part of analysis programs in certification of aircraft. To increase correlation between test and simulation, filtering can be applied to analysis data to eliminate unnecessary data. According to the authors, simulation is beneficial for developing structures[6]. However, they believe that simulation capabilities are not sufficient at this time to achieve crash certification by analysis.

At NASA, same researchers conduct another study to evaluate test/analysis methods. Two drop tests of the section were made. The work concentrated on the test and simulation results for an advanced concept full scale fuselage section. The accuracy of the model correlation depends on the accuracy of the global stiffness and mass distribution for the finite element model[6]. In these cases, there exists little opportunity to evaluate data quality for correlation with crash simulations. Evaluation of the crash finite element simulation accuracy requires the comparison of results in several

formats[25]. Filtered time history accelerations and velocities enable evaluation of correlation details. However, the significant variations between even symmetrically located positions make meaningful quantifications of the reasons for the discrepancies include: geometric defects, material variations and inaccurate estimate of the impact conditions. Measured and predicted data can be compared with peak acceleration, dynamic response index and weighted average[26]. These approaches allowed evolution of the significance of scatter in the time history data in combination with factors such as duration, peak acceleration, onset rate, frequency content, and mean.

2.4 ABAQUS Finite Element Model

Finite element programs have become more important on design and analysis of aircraft structures in orded to improve crashworthiness of the structure. Even though experiments give much better results than analysis, with high costs and long data processing times, the necessity of the software programs increases[6]. It is very expensive to create even a single model, yet it is impossible to create hundreds of test specimens and optimize structure. In addition, specimens are nearly ruined after initial buckling. After that point, it is very hard and the complicated to collect accurate data. So, finite element programs are developed especially on crash analysis for test correlation[7]. Crash is a non-linear dynamic problem. Because of the non-linear nature of the crash event, a dynamic/explicit solver is required. ABAQUS Dynamic/Explicit has ability to perform dynamic crash test in computer environment. Since high deformations occur, self-contact of the specimen happens. This is another aspect that increases the problem complexity. In the model, three-dimensional shell elements are used as a test specimen. Rigid elements are used at the ground and drop mass parts. Rivet is modelled by fastener modeller feature. Material plasticity is highly important to simulate the test results. Optimization code will communicate with ABAQUS script. This script is compatible with MATLAB and LS-DYNA. Thus, it enables us to run the genetic algorithm in different programs to find the optimum solution.

ABAQUS/Explicit solver is used because analysis is nonlinear, dynamic and it includes excessive contact. Explicit solver manages nonlinearities easier than implicit

analysis. Trial solution is needed to find equilibrium in implicit analysis but explicit analysis solves directly. Since dynamic analysis includes mass/inertia and damping effect different than static analysis, complexity of the problem has increased.

Explicit solver has many advantages over implicit analysis. Explicit solver uses element mass matrices instead of using complex stiffness matrix that inversion is expensive. At the end of each increment, explicit solver recalculates the mass matrix according to geometry and material changes. The next increment of load is calculated based on new stiffness matrix. The disadvantage of this method is that small increments are needed which is time consuming. Euler time integration is not used so analysis is unconditionally stable. Bigger steps move away from correct solution. Despite long analysis duration, explicit solver is essential to solve this type analysis.

2.4.1 Analysis Solver

In nonlinear analysis, a geometry and material requires incremental loading steps. Geometric and material changes are reconsidered. Solver update the solution matrix. Implicit solver uses Newton-Rapson iteration to reach equilibrium. Implicit analysis is more accurate then explicit analysis. It can solve problem with bigger steps. In explicit analysis, solution depends on size of the increment. The result will drift from correct solution if the iteration size is not sufficient. For different time increment size, final shape of the solution will be different. The suitable type of analysis depends on problem type. Since crash analysis include high nonlinearity and dynamic equations, problems generally computationally intensive. Explicit solver shows better performance on high nonlinear dynamic problems.

2.4.2 Contact Modelling

Two bodies sliding is modelled with respect to each other. Two possible approach are available in ABAQUS contact modelling: defining possible contact surfaces and using contact surfaces. With the first method, contact elements generated by finite element solver. In this study, contact surfaces is defined. One of the surfaces is defined as the slave surface and the other surface is the master surface. The master surface is defined

as slide line. There are two slide lines which are linear and quadratic segments. These slide lines are shown in figure... Surface folding and touching itself is accepted as self-contact. The theory is same for self-contact.

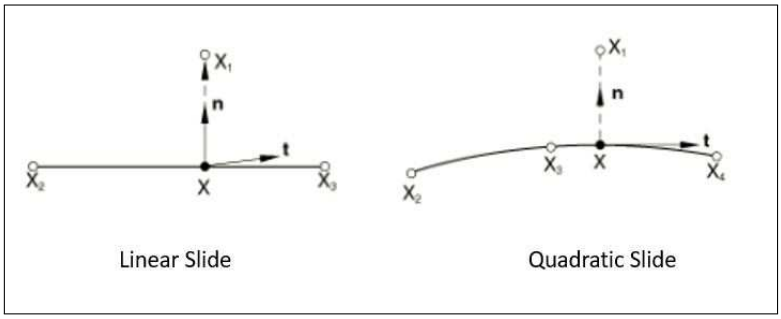

Figure 2.1: Slide Types

2.4.3 Shell Element

Specimen can modelled with either solid elements or shell elements. Convergence of analysis with solid models are harder. The required time is also more compared to shell analysis. To find optimum solution, hundreds of analysis conducted. Thus, shell element modelling is better choice for this thesis. In ABAQUS library, there are general purpose, thin and thick shell elements. Classical shell element theory is applied for thin elements. Shear Flexible shell theory is applied to thick shell elements. General purpose shell element can use for thick and thin parts. ABAQUS/Explicit has only general purpose shell elements. S3, S4, S3R, S4R, S4RS, S4RS and S4RSW are three-dimensional shell elements of ABAQUS. S4R element is used in this research.

In ABAQUS/Explicit, 'effective section Poisson's ratio' is used to calculate thickness change of shell elements under large deformation. The thickness change based on this method is calculated as follows.

Linear stress gives in plane stress, $\sigma_{33} = 0$

$$\epsilon = -\frac{\nu}{1-\nu}(\epsilon_{11} + \epsilon_{22}) \tag{2.1}$$

Treating these as logarithmic strains,

$$\ln(\frac{t}{t_0}) = -\frac{\nu}{1-\nu}\left(\ln(\frac{l_1}{l_1^0}) + \ln(\frac{l_2}{l_2^0})\right) = -\frac{\nu}{1-\nu}\ln(\frac{A}{A^0}) \tag{2.2}$$

Symbol A refers the area on shell surface. The nonlinear thickness relationship becomes,

$$(\frac{t}{t_0}) = (\frac{A}{A_0})^{-\frac{\nu}{1-\nu}} \tag{2.3}$$

For $\nu = 0.5$, the material is incompressible. If it is equal to 0, the thickness does not change.

CHAPTER 3

METHODOLOGY

A strategy for the optimization process is shown in block diagram. In figure 6.13

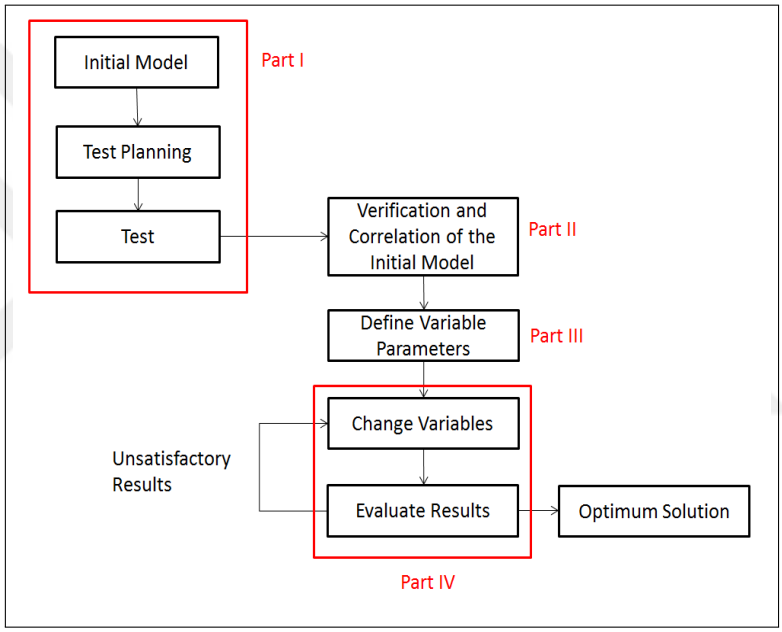

Figure 3.1: Strategy Flow Chart of Optimization Process

3.1 Test Part

The whole part 1 is taken from another study. In the thesis, opportunity to conduct test is very low. Crash tests are very expensive and very hard to perform. These kind of tests are very complex to get an effective result and to interpret it. Thus, first part is taken away from a previous research. AGUSTA helicopters studied about their new subfloor intersection element's energy absorption capability. To get a result, they

conducted experimental and numerical investigations. Correspondingly, they conducted a research with Politechnico di Milano University. Energy absorbing design of AGUSTA helicopter is investigated. Bisagni published a paper on this study which is crashworthiness of helicopter subfloor structural component[10]. Study focused on subfloor structural intersections. The reason of the study is to detailed subfloor structure and to understand energy absorbing mechanism. At this paper, simple floor intersection element is tested. Finite element model is also used to simulate crash. Both finite element programs and hybrid programs are used such as, ABAQUS/Explicit, PAMCRASH, KRASH (Lockheed) and VEDYAC (Politechnico di Milano).

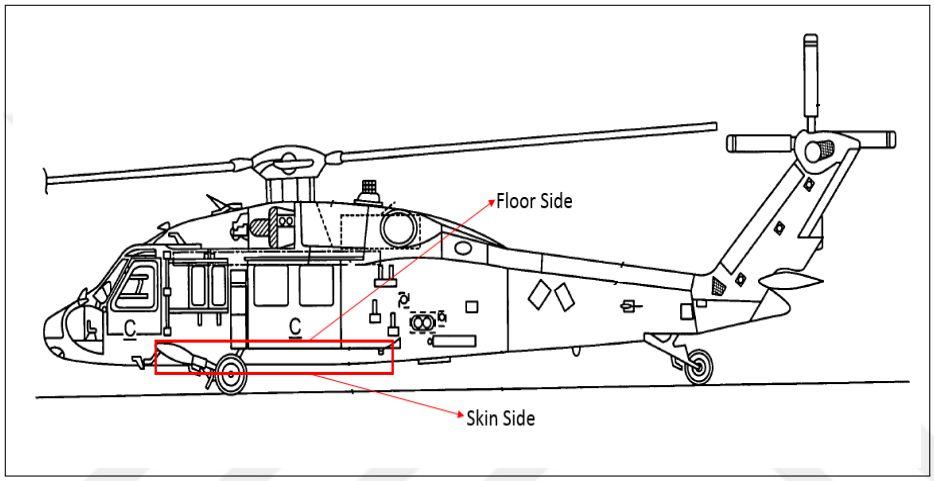

Figure 3.2: Subfloor Region of Helicopter

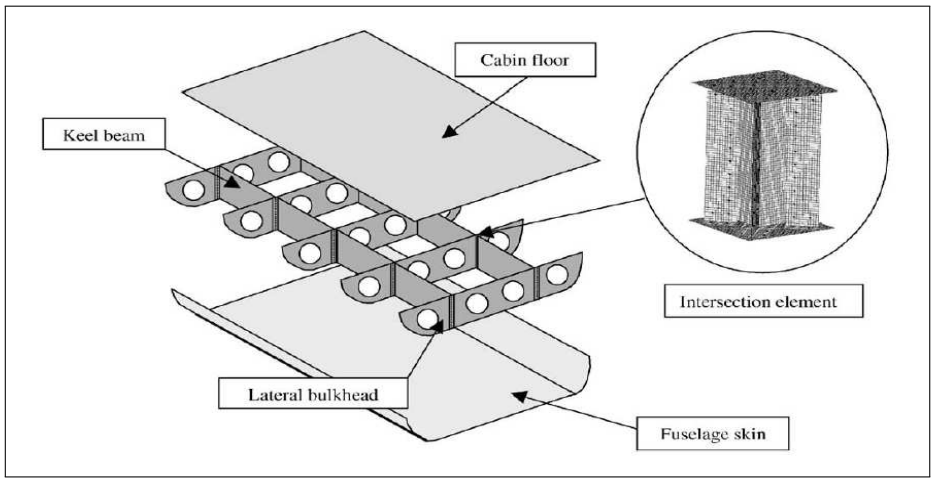

Figure 3.3: Example of Floor Intersection Element

Initial model is riveted structural intersection element. Height of the section is 195mm. Section has two vertical webs and four angular elements. These elements formed

close square section. There are two plates, which are bases, enclose specimen from the top and bottom.

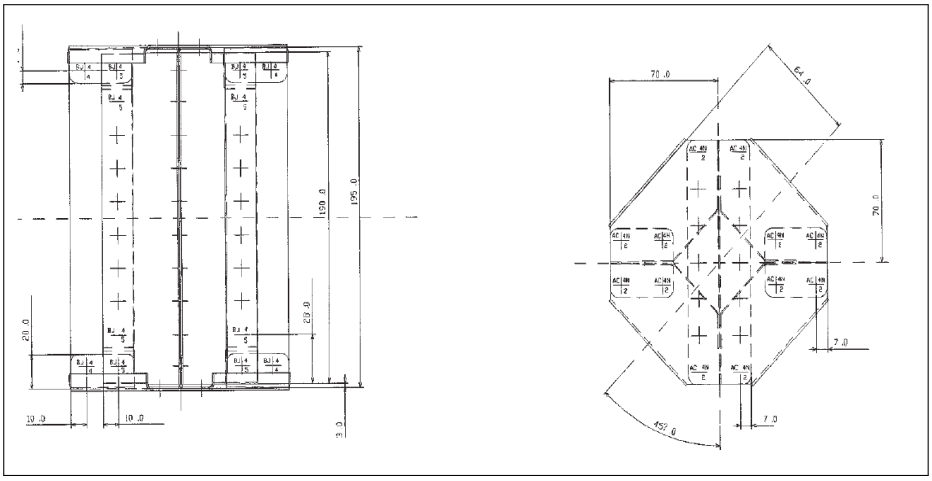

Figure 3.4: Dimensions of Test Model Specimen

All these components are attached to each other by eight small L-shaped brackets. The thickness of the bases are 1.27 mm each. The thickness of each remaining part is 0.81 mm 2024 T3 aluminum alloy is used for all parts. MS20470 and MS20601 rivets are used as fastener. Assemblies are given in figure 3.4 and figure 3.3.

At experiment, drop test machine is used. Test is recorded with high speed camera. Displacement of the test specimen and acceleration of the mass are recorded. 110 kg mass is impacted a specimen with 7 m/s. After the test, needful data is collected. The diagrams are analyzed and interpreted. One of the significant results is peak load which is maximum force of the load-shortening diagram. The other results are average crush load, absorbed energy, and specific absorbed energy and crush load efficiency. At the experiment, the measured peak force is about 52 kN. The average crush load is between 25.5 to 28 kN. Specimen's absorbed energy amount is 6.5 kJ/kg. Experimental and numerical results are collected from the study are given in figure 3.5.

3.2 Verification and Correlation of Initial Model

This part is done with finite element program. On the paper, crash is simulated with finite element. In this thesis, verification of the test setup is done one more time to get

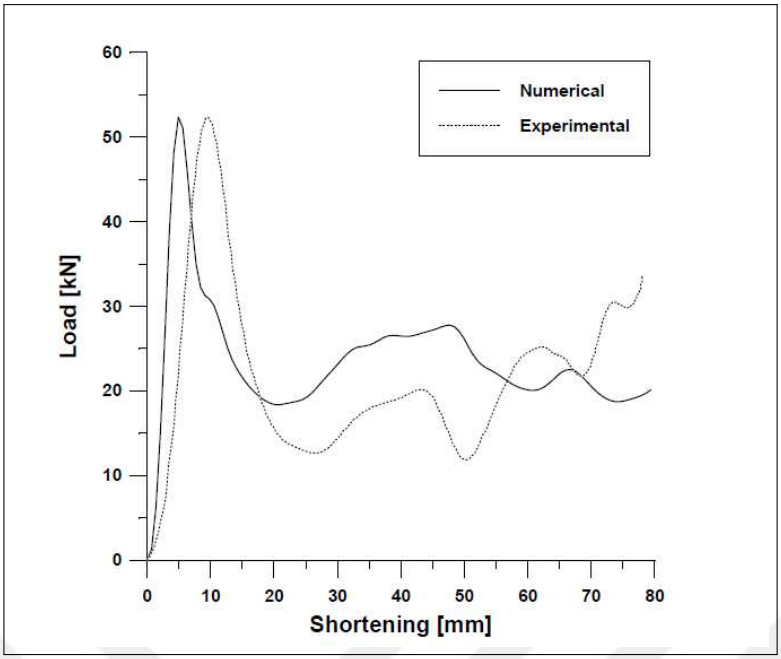

Figure 3.5: The Comparison between Experimental Result and Numerical Result

similar data with research paper. After verification, optimization has started. The idea is that if the test setup model is created accurately, optimum result could be found by changing variables without the test. The key point is simulating the test as accurate as possible. Then we can trust model even at different dimensions. To get more accurate result on optimization, analysis model should be similar to the test specimen as much as possible.

In this thesis, ABAQUS/Explicit code is used to verify test. Structure is modelled as a four-node shell element. The initial model has 21 600 elements, 22 690 nodes. Elements and nodes have 6 degrees of freedom. 2024 T3 aluminium alloy is assigned to parts. Stress-strain curve of aluminium is given in chapter 6.2. Both elastic and plastic properties of material are assigned. ABAQUS uses Von-Mises isotropic plasticity algorithm. In reference paper, aluminium alloy strain sensitivity is defined according to the Cowper-Symonds formulation. The formulation is [10],

$$\sigma(\epsilon, \dot{\epsilon}) = \sigma_0(\epsilon) \left[1 + (\frac{\epsilon}{D})^{\frac{1}{p}} \right] \tag{3.1}$$

In the finite element formulation, since intersection elements sustain high deforma-

tion, several contact algorithms are defined. Self-contact is defined to eliminate interpenetration between each structure surface and itself. Each part penetration is prevented. Penalty formulation is used for all contacts. Counter forces at contacting surfaces are increased proportional to penetration depth.

Rivet modelling is also important for the subject. It is very complex to simulate rivet failure under dynamic load. Rivet has many failure modes such as breaking of rivet, pullout of rivet and breaking. To simulate rivet, ABAQUS fastener tool is used. In our topic, failure mode of the rivets is accepted irrelevant. Energy absorbing capacity of whole structure is our main concern. Bisagni also investigated stiffness of the rivet. Analysis is solved with both rigid and elastic rivets. The results are compared. Rivet stiffness has no influence on energy absorption capacity[10]. That's why rigid rivets are used in our finite element models.

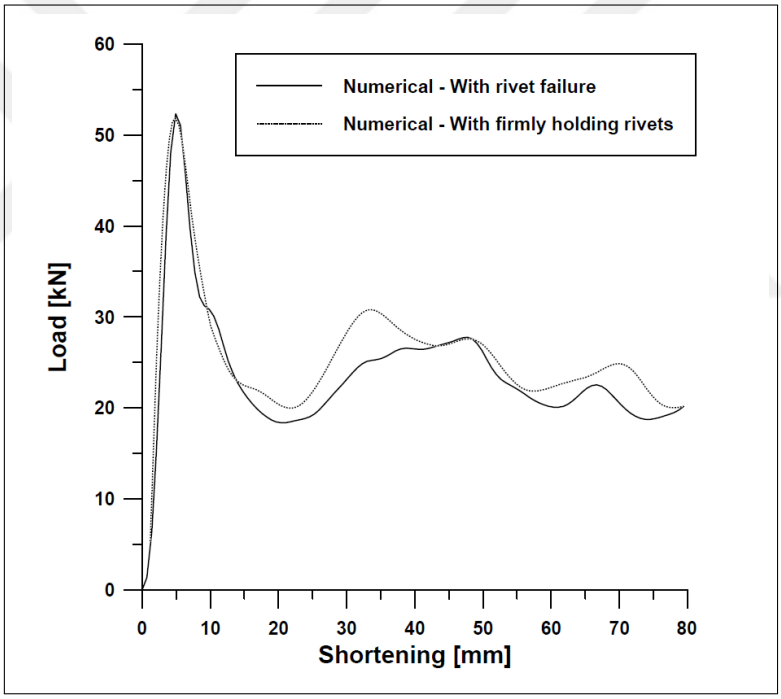

Figure 3.6: The Effect of Rivet Type on Analysis Result

3.3 Design Parameters Definition

Defining design variables is crucial to shorten optimization process. Assembly consists of 16 parts. Each part dimensions could affect energy absorption more or less.

Thickness, width and length could be changed to understand its effect. Lower and upper boundaries are also effecting optimization time. Step size between limits have influence upon period of analysis. This process is critical because it directly affects optimization duration[29]. Intelligently chosen variables decrease unnecessary effort.

According to literature, upper and lower bases have small influence on energy absorption[30]. Bases are parallel to crushing direction. As we stated in literature review part, element which is perpendicular to crushing direction has small influence on structure deformation. Assembly has 8 brackets to connect beam to angular elements and bases. Bracket's vertical height is very small. Upper L-parts buckle insufficiently. That's why L-parts have very small contribution on energy dissipation. Even their contribution is expected small, their thickness and material are also added as variable to evaluate results. Keel beam dimensions are also determined by optimization. Keel beams are main energy absorber for helicopter subfloor structure. Beam and frame thicknesses have high importance on energy dissipation. The main reason is to optimize intersection element to find better angular element. This angular type intersection is a new design. This design is used to absorb crash load. This type of intersection could absorb more energy by changing length, width and thickness. In this thesis, main design object is angular element. In optimization part 2, material is added as another variable. It is applicable for angular elements and L brackets. It is very expensive to use titanium and magnesium for beam, frame and floor so it is not feasible. That's why titanium and magnesium are design parameters for bracket and angle.

3.4 Optimization

As stated before, the main aim is to find better shape of angular element. Height of the upper bound is height of the bulkheads. It is a physical limit. Lower boundary of the angular element height is set as half height of bulkheads. For thickness, standard thicknesses are used. In 2024 T3 sheet aluminium, only certain thickness sheets are produced. These thicknesses are 0.6, 0.81, 1.0, 1.27, 1.42, 1.6, 1.8, and 2.0. 2.0 mm thickness is chosen as upper limit because sheet metal is generally not produced higher than that value. 2.0 mm is the maximum catalogue thickness. The design

variables are given in figure 3.7.To connect two sheets with rivet, sheet thickness should be higher than 0.6 mm. Thus, thickness boundaries are set to these values. The optimum energy absorbing intersection element is found by changing these values.

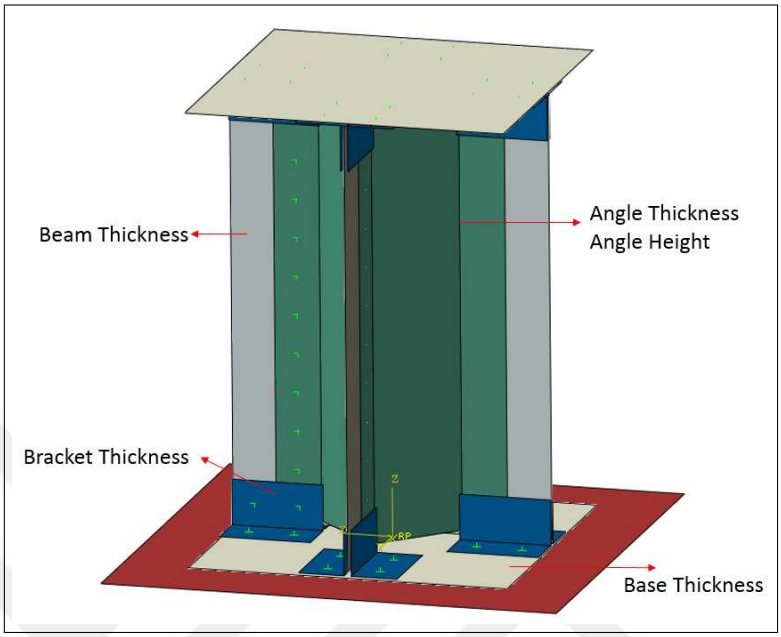

Figure 3.7: The Optimization Variables

To evaluate collected data, several measurements, calculations and diagrams could be compared. This could be deformation shapes. Since analysis is nonlinear and explicit, deformation has small differences for each analysis. Generally, FE correlation model have imperfections at intended place[31]. That's why tester can get similar deformation shapes. In optimizing process, we are not using imperfections at any place of specimen. Thus, energy absorbing results should be compared rather than deformation. These results are peak loads, average crushing load, absorbed energy, stroke efficiency and crush load efficiency. The most important optimization aims are decrease the peak load and to increase energy dissipation during crash.

The longest and the most critical part is iteration process. In iteration, parametric code is needed which should run perfectly every point within the bounds. That's why parametric code is the most important part in optimization. Then this model script and optimization code are combined. In optimization, it is very easy to mistakenly converge local minimum. To avoid local minimum points, optimization algorithm

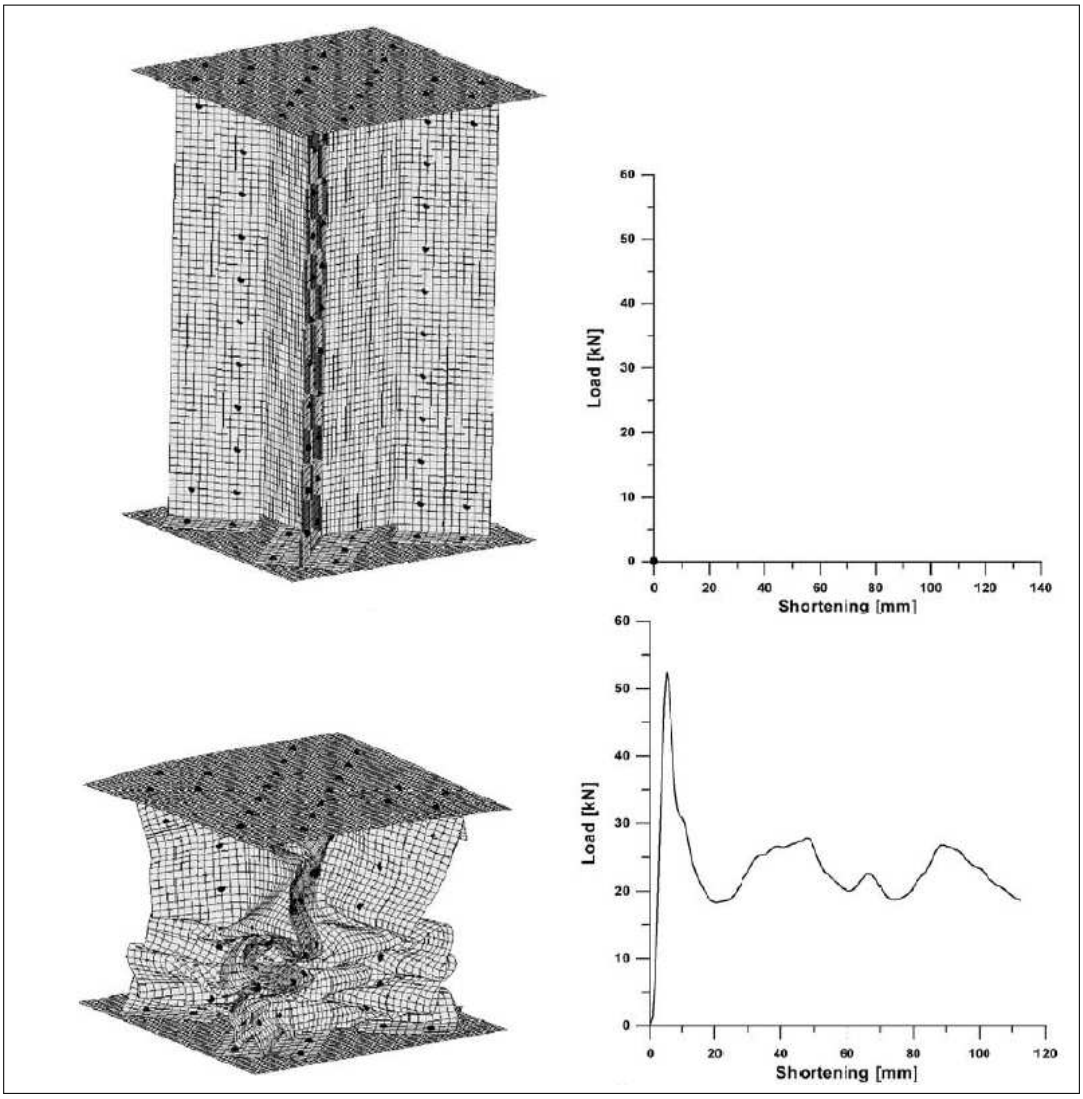

Figure 3.8: Initial and Final Specimen Shapes from Research Paper

should work wisely. To do this, D-optimal design will be used. With intelligently selected points, our variables keep away from local minimum and converge to global minimum result[32].

To find optimum solution of design problem, one of the optimization methods should be selected. Then objective function has to be defined. The objective function of our problem is minimizing peak load. Displacement constraint is not exist for this problem. The reason is that if the specimen deforms to much, the stiffness of the specimen will increase and higher reaction force will be developed. Thus, displacement constraint is irrelevant. For design variables, constrains have to be determined. Physical boundaries are going to designate thickness and height limits. Genetic algorithm is chosen as optimization algorithm.

At 1950s, scientists have studied on computer programs which could imitate natural reproduction and mutation. Studies start to create artificial intelligence then evolve to create optimization code[33]. Genetic algorithms can check all solution space instead of focusing on single solution and work with complex data. Genetic algorithm is simulating of biological process so terminology is used from biology. Genetic algorithm is a very good optimization method option for complex search problems. This method is generally used to create high quality designs. It has many benefits over classical algorithm. Classical algorithm generates a single point to approach solution. However genetic algorithm, starts from population of possible solutions. The best point approaches to the best solution. Classical algorithm uses deterministic computation to select next point. In genetic algorithm, random generators are used. Genetic algorithm is applicable to problems that are not fitted to standard optimization methods. Discontinuous objective function, non-differentiable and highly nonlinear problems can be solved with genetic algorithm. This method is applicable for huge combination of parameters to find the best solution. Genetic algorithm can solve schedule tasks and computer problems. Genetic algorithms work similar with evolution process which is natural selection in nature. Although the method is used in very complex problems, it is very simple to understand.

The method takes fundamental rules of natural selection and applies these rules into the problem. The method has six steps. These are initialization, evaluation, selection,

crossover, mutation and repeat. At first step, initial population is randomly generated. The number can be from few to hundreds. Secondly, each result is evaluated and 'fitness' of all individuals are calculated. This calculation is depending on wanted requirement. Then selection step comes. To improve design solutions, bad designs should be discarding. There are a couple of different selection methods to discard bad designs but the idea is the same. In fourth step, new inputs are created from selected results. The idea is that by combining better solutions, the fittest solution can be found. The fifth step is mutation. To get rid of local best solutions, randomness should be added into population. Otherwise, all combinations are created from first population. Mutation can provide diversify populations' variation by making small changes. Then final step is over again. By starting from step two, more different and finer result can be found. Termination depends on predefined minimum criteria. If the results come close to each other, it is likely to find the fittest result. Although all of the optimization methods cannot guarantee to find global minimum, genetic algorithm is likely to escape from local minimum. That's why genetic algorithm is one of the best options to optimize these crash optimization problems.

After optimum thickness and length of the design variables are found, the effect on energy absorption capacity and initial peak load are shown. If the results show other than what is found in literature review, new variables are added to optimization problem. MATLAB Optimtool is used for optimization. Variables and boundaries are given as an input then MATLAB generates random numbers for creating populations. After analysis is conducted, outputs of ABAQUS become input for MATLAB then vice versa. There is another code for doing this job which creates connections between MATLAB and ABAQUS. With this codes, iterations are made and optimum solution has been found.

CHAPTER 4

FE MODEL - TEST CORRELATION

4.1 Geometric Properties

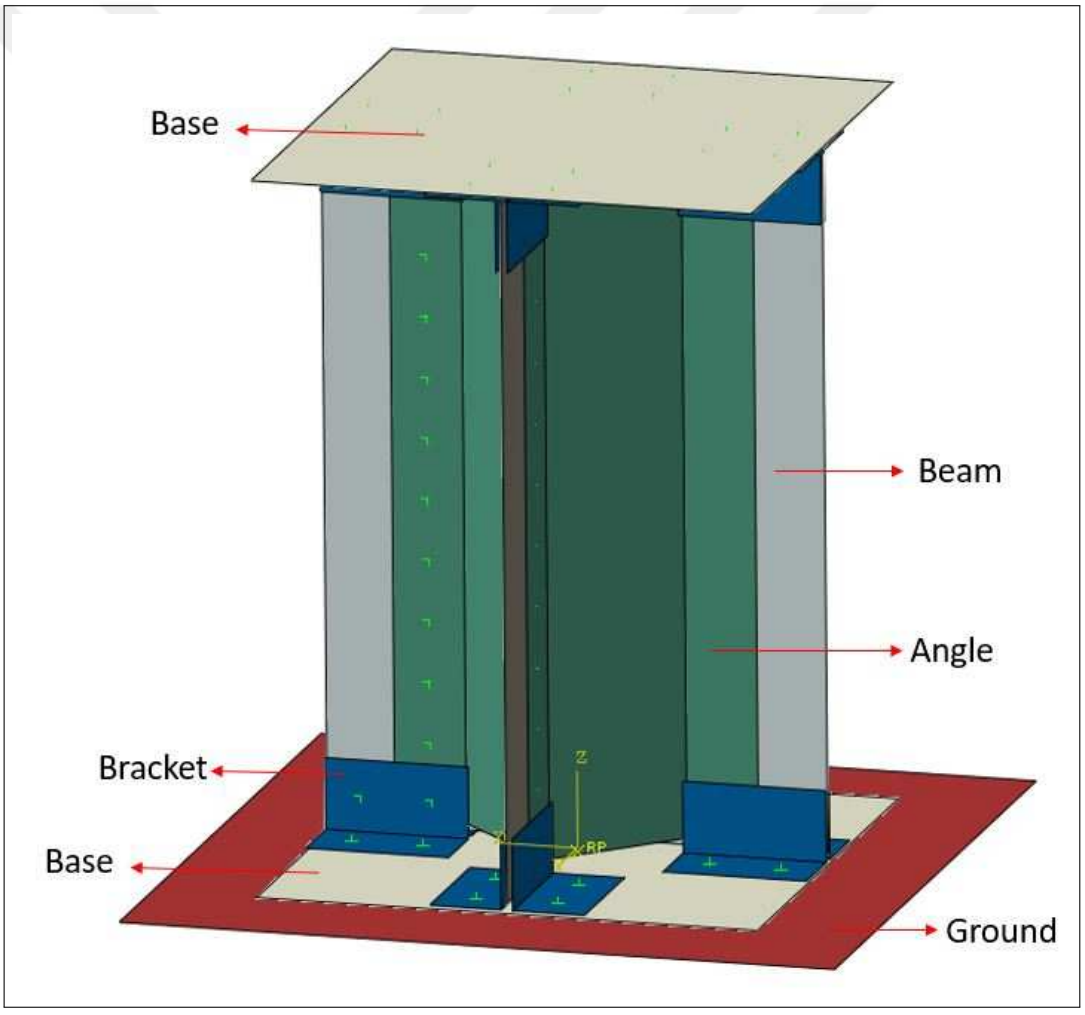

Figure 4.1: Test Model FE Assembly

Assembly consists of 25 distinct parts. These are 16 L brackets, 4 angles, 3 beams

and 2 bases. Total height of the specimen is 195 mm. Angle height is 190 mm. Only upper base and lower base thicknesses are 1.27 mm each, remaining parts thickness is 0.81 mm. Parts are detailed in the figure 4.1. Mass and ground modeled as rigid part where specimen compress between them. Reference point is created on rigid mass part and 110 kg mass is tied to this point. Specimen comes into existence by assembling all parts together. Thus, clearance between ground and specimen bottom side is zero. Likewise, clearance between mass and specimen top side is also zero. All parts are modeled as shell element so thickness is assigned as a property. According to their thicknesses clearance is arranged.

Green dots shown on assembly plot are fastener locations. 4 mm diameter fasteners are used. Spacing between rivets are arranged as 5d which is 20 mm. Rigid fasteners are used. The main aim in geometric modeling is to create identical specimen between test setup. Specimen is crashed between punch and die which are much stiffer than test specimen. These parts are accepted as rigid in our model which are ground and mass. It can be said that test and model geometries are identical.

4.2 Material Properties

Aluminum 2024 T3 material is used for all parts. Stress-strain curve of material is given in figure 4.1. A plastic property of material is also assigned to FE program. Necessity of the material plasticity is related with degree of deformation. Linear elastic material is easy and faster for small deformations which returns to original shape after loading. High loads like crash create permanent deformation on material. In this case, linear assumption is not valid. The permanent deformation means dissipation of energy that irreversible and path dependent. Crash load leads to excessive deformations so elastic strain neglected. Plastic region has become main concern. Cross sectional area change is large enough to affect finite element analysis result. Thus, material model and geometrical nonlinearities should be included in such analysis. Because of high deformation, rate dependent plasticity Cowper-Symonds formulation is defined which was given in Eq. 3.1. With this formulation strain rate sensitivity is added to analysis.

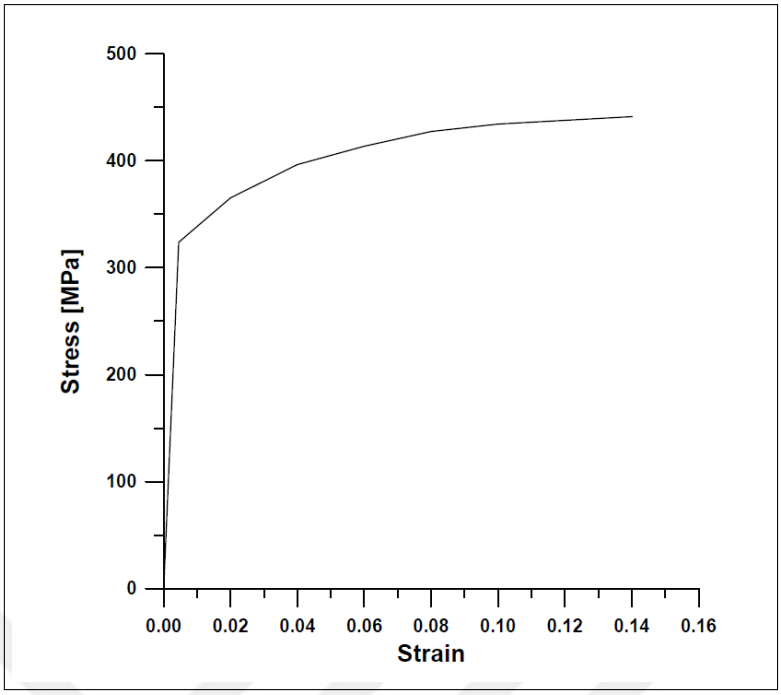

Figure 4.2: 2024 T3 Aluminum Alloy Stress-Strain Curve

Table 4.1: The Mechanical Properties of Aluminum 2024 T3[35]

Young Modulus	E	70 GPa
Yield Stress	σ_y	326 MPa
Yield Strain	ϵ	0.001
Poisson's Ratio	ν	0.3

During analysis, geometric non-linearity is considered. FE solves analysis with load increments. After each load increment, geometric dimensions are not updated at linear geometry. However nonlinear geometry has ability to identify size, shape and position changes with load increment. It is essential at high deformations. As a rule of thumb, geometric nonlinearity should turn on when strains are higher than 5%. Crash analysis includes excessive deformations so it is necessary to get an accurate result.

4.3 Geometric Imperfections

In real specimens, different than FE model; there are imperfections such as cracks and surface defects. These dissimilarities prevent demonstrate real structural behaviour

at FE programs. Moreover, when load is applied, finite element can apply perfect compress but in real case buckling occurs. Because of these reasons, there could be differences between model result and real case result. Imperfections are not defined in the rest of the correlation part.

4.4 Load and Boundary Conditions

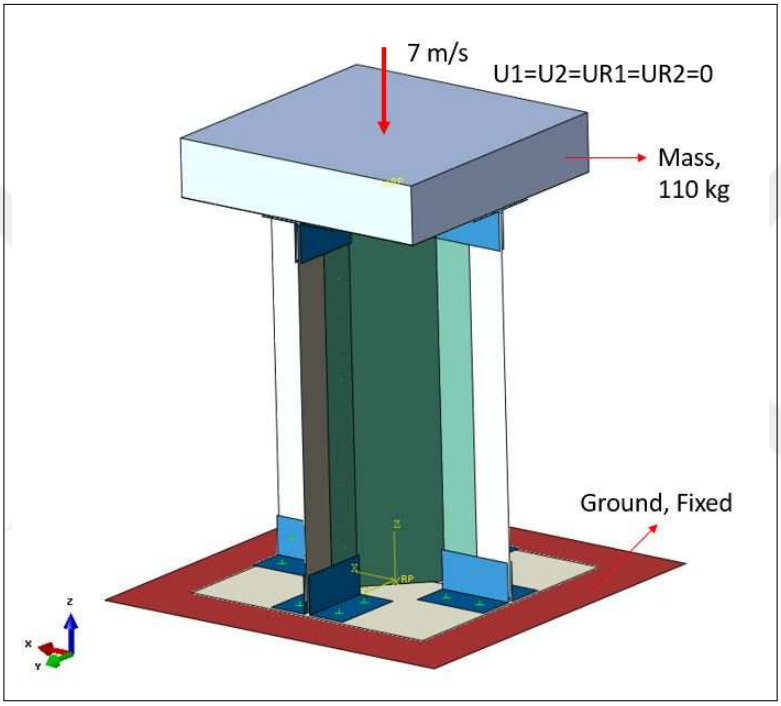

Figure 4.3: Boundary Conditions and Load of Analysis Specimen

Bottom base is fixed in all directions but mass plate fixed all except translation and rotation in -z axis. The mass hits specimens top edge, z-translation free to simulate crush sequence. Figure 4.2, shows the bottom and mass parts of assembly. The impact controlled 110 kg mass and 7 m/s velocity. Even contribution is very limited; gravity is also added to the model.

Table 4.2: Boundary Conditions of Analysis Specimen

Part	X-Translation	Y-Translation	Z- Translation	X-Rotation	Y-Rotation	Z-Rotation
Bottom Base	0	0	0	0	0	0
Mass	0	0	Free	0	0	Free

4.5 Result

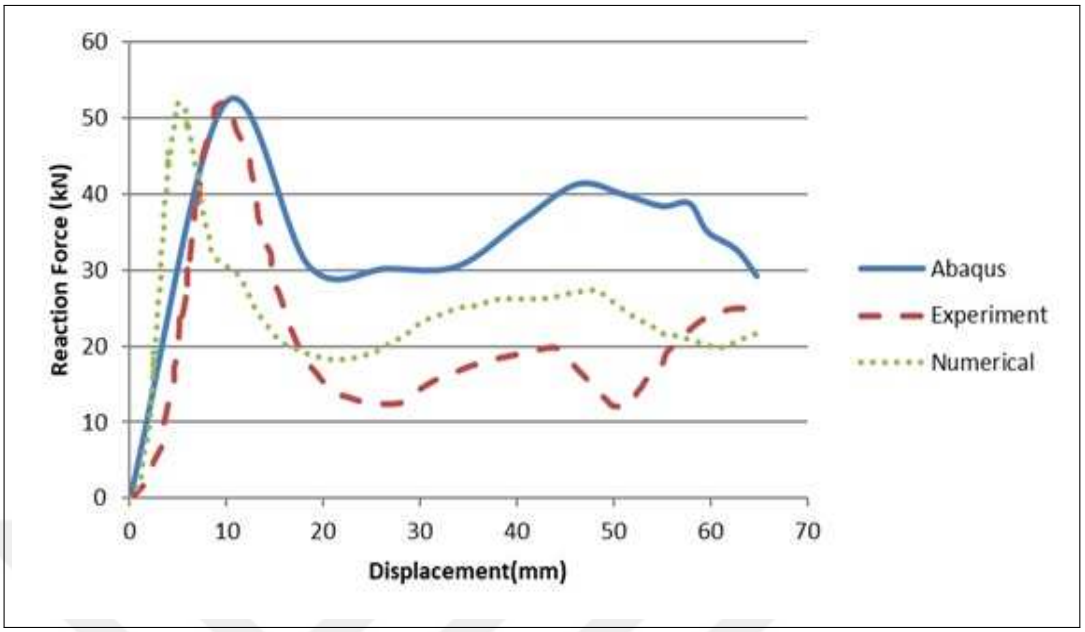

Figure 4.4: Comparison of Test Result, Numerical Result and Thesis Model Result

In figure 4.4 , we can see load - shortening diagram of ABAQUS analysis result, experimental result and numerical result. Experiment results are taken from another research paper [10]. At load-shortening plot, elastic region continue up to a curve peak load, then load is decreased sharply down to 25 mm deformation. Curve up to peak load is linear, after that point non-linearity has started. High degree of accuracy is expected at elastic region. After each buckling, reaction force is decreased because section goes in post buckling forces. Buckling at force-displacement curve is local not global. At each buckling, local part of the section developed load and buckle, then another part of the specimen start to compress and buckle.

As we can see from Ideal Load - Shortening Curve from chapter 2, our main aim is to decrease the initial peak load as much as possible. In graph, our result conformity is very close to experimental result. Initial peak load is found the same. Although numerical result approaches peak load abruptly, our result approach top point is more inclined which is similar to the experiment. After initial 20 mm shortening, disparity has started. Numerical result and FE result cannot decrease as much as experiment result after initial buckling. In experiment, second buckling occurs before FE and numerical result. These are related with limited modeling of material and fasteners.

In finite element programs, materials are stiffer than real case. After peak point, non-linearity and geometrical effects increased, the accuracy of the result reduced. Another reason of this difference could be element choice. 4 node elements are poor in bending[34]. Time steps can also affect difference between test result and analysis. The other parameters to compare results are given below. Total dissipated energy, specific absorbed energy, peak load and average crushing forces. Area under the load-displacement curve gives total absorbed energy. To compare energy absorption capacity of each structure, reaction force-displacement plot can be compared.

$$P_C R = \frac{\pi^2 EI}{(KL)^2} \tag{4.1}$$

Table 4.3: Mass of the Structure

The mass of the structure(kg)	
Angle (x4)	3.43e-2
Bases (x2)	6.72e-2
Bracket (x16)	0.35e-2
Long Beam (x1)	5.90e-2
Short Beam (x2)	1.68e-2
Total Mass	42e-2

The specific absorbed energy= $\frac{2.695}{42e-2} = 6.41 kJ/kg$

The peak load is found as 53 kN. This value is nearly same with the test. This means buckling is modeled very close to the test. The area below load-shortening diagram also gives absorbed energy. The area found in 2.5 kJ. This is also very close to total energy of impact.

The average crush load is found as 33.5 kN. The average force is calculated by dividing the area under force-displacement diagram by the shortening of the specimen. This is a bit different than test result. The average crush load is found higher than the test result which is found in numerical calculation. The reason is finite element programs cannot model exact material deficiency. Analysis programs use material as a perfect aluminium. Material defects ease buckling of specimen. In finite element model, since material cannot buckle easily, higher forces are generated. This increases the average crush load. Stroke efficiency is the ratio between final short-

ening to initial length. Stroke efficiency is higher at test specimen. Test specimen deforms more than finite element model. The reason is the same with average crush load difference. The defects at material can increase deformation. Since modeled materials are perfect, assembly is stiffer at finite element model. Because of the same reasons, crush load efficiency is higher at finite element model. The most important parameters are peak load and absorbed energy. These are two parameters to correlate model. Peak load and absorbed energy are very close total results. As a result of this outcome, we can say that finite element model is similar with the test. Peak load is matched better than remaining parts.

In correlation, presented results showed similarity with test more than research paper's result. ABAQUS found closer results at the beginning of crash. The maximum peak load is our initial design object. That's why resemblance between tests at the first part is more crucial than the remaining part. Deformation shapes of ABAQUS result and research paper results are compared below. The deformation results are compared for initial buckling, second buckling and final shape. These are the main buckling shapes of whole structure. We can state that deformation shapes are very close to each other. As a result of this comparison, our analysis results are very close to test and paper results. Thus, we can say that our model is correlated.

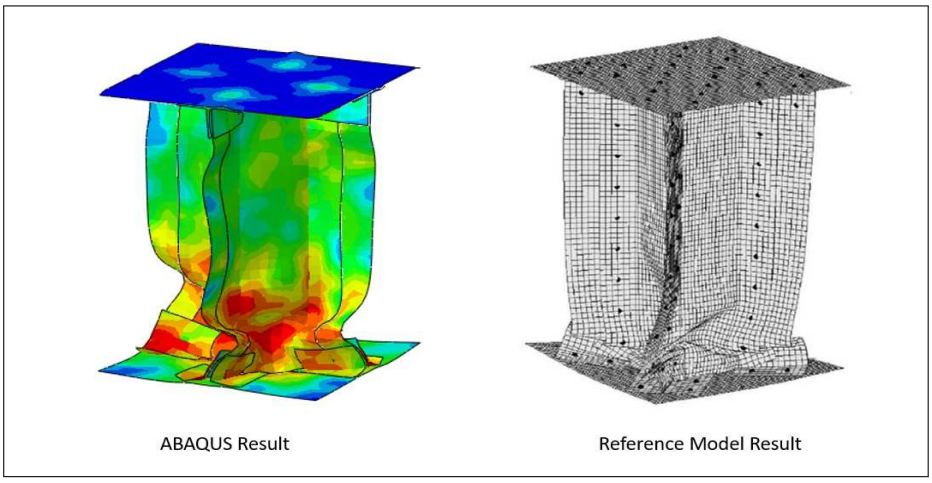

Figure 4.5: Deformation of Thesis Model Result and Research Paper Result at Initial Buckling

Figure 4.7 - Deformation of Thesis Model Result and Research Paper Result at Ini-

tial Buckling shows shape of specimen when it reaches peak load. After that point, structure continues its deformation. Stresses at the outer edges start to decrease with increasing displacement. Then, stress starts to concentrate on joining intersection region. In Figure 4.6 - Deformation of Thesis Model Result and Research Paper Result at Second Buckling stress has developed the center intersection element.

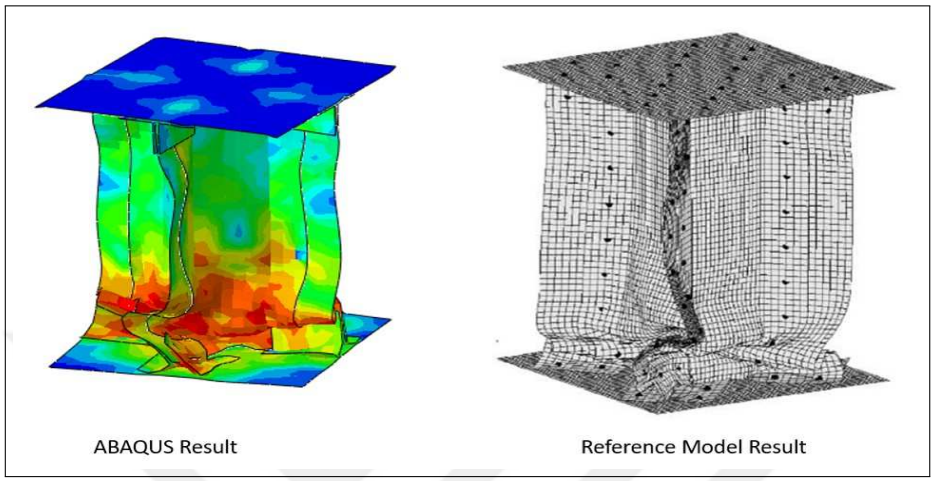

Figure 4.6: Deformation of Thesis Model Result and Research Paper Result at Second Buckling

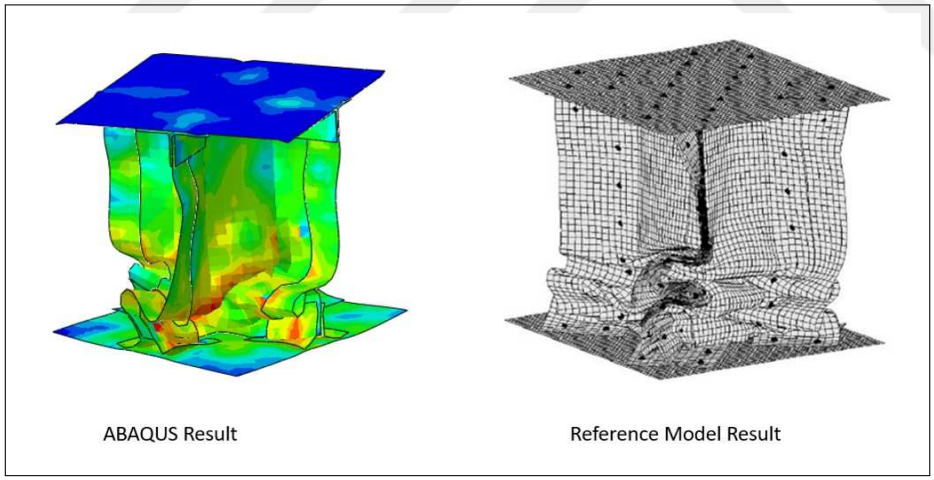

Figure 4.7: Final Shape of Thesis Model Result and Research Paper Result

Result obtained in ABAQUS model generally agreed with the test result. In modeling, knowledge of elements, boundary conditions and modelling contacts are not fully known. Thus, differences could always occur between analysis and test. The aim of this part is correlated test with FE; it is considered that required data is good correlated between test and analysis.

CHAPTER 5

OPTIMIZATION - PART 1

5.1 Optimization Theory

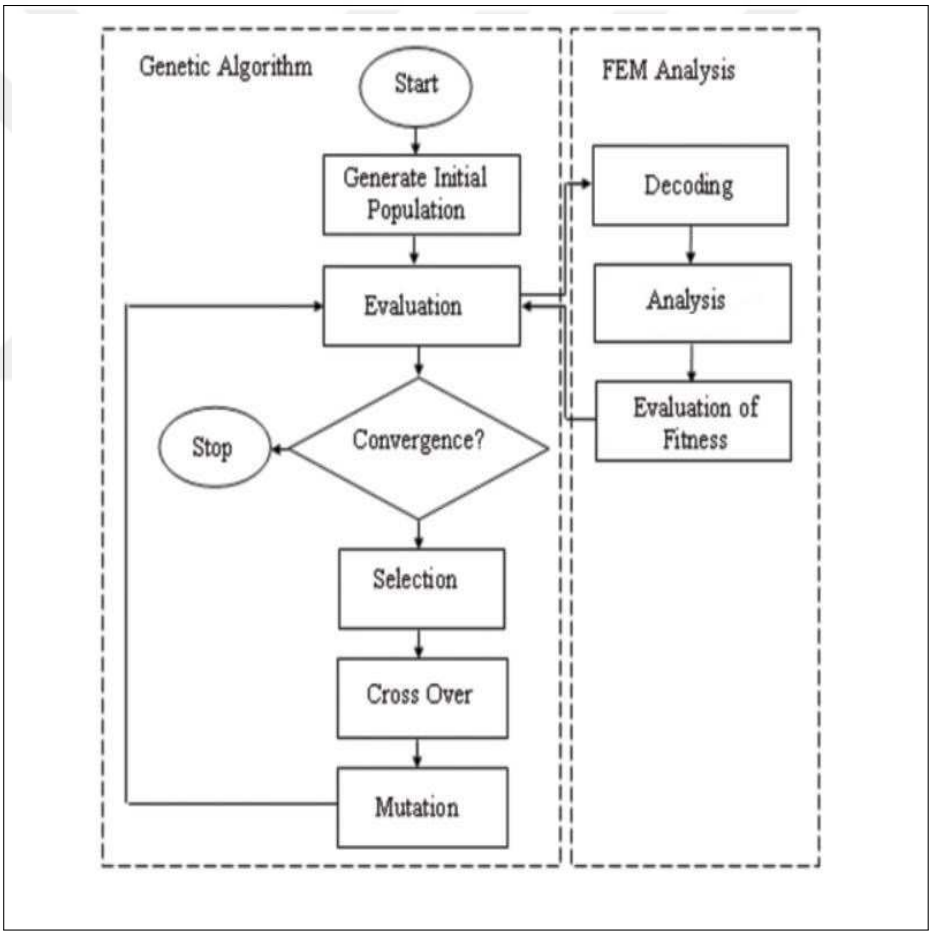

Figure 5.1: Genetic Algorithm Procedure

In first part, whole structure material is aluminium. Material is not a design variable. Design objects are angular element thickness, angular element height, beam thick-

ness, L bracket thickness and base thickness. To optimize these variables MATLAB Optimtool is used. Optimtool create random inputs then evaluate results. According to results, some inputs are eliminated, some of them survive. As explained in previous chapter, analysis is solved via ABAQUS with python code. Thus, another connection code is needed for communication between ABAQUS and MATLAB. This code copy input files which is created by MATLAB and write into ABAQUS input file. After analysis is finished, copy required finite element result to MATLAB. Consequently, MATLAB generates new input files and optimization process keeps on continue.

Optimization procedure is given in figure 5.1. At evaluation part, analysis of all population's analysis is finished. After that section, tool checks whether genetic algorithm is converge. For this problem convergence criteria is determined as 10 iteration. Algorithm creates new individuals until 10th iteration. Optimtool generates integer numbers, but thickness values are not integer. Input values are discrete not continuous either. To solve this problem, array is required to create input file from MATLAB. Array for thickness and height is given below,

Table 5.1: Domain of the Variables (Optimization Part 1)

Variables	Variable Domain
Thickness	0.6 0.81 1 1.27 1.42 1.6 1.8 2
Height	100 105 110 120 ..... 185 190

Boundaries of arrays are defined to Optimtool. MATLAB generates five integer numbers for five design variables, then inputs values are copied to python file as an ABAQUS input. After analysis is finished, maximum value of reaction force-displacement curve is copied to MATLAB. Then, new generations are created and same procedure is repeated.

Initial population variety is ensured with randomly chosen individuals. Then each individual is evaluated according to fitness values function to examine how well it solves the problem. Selector operator eliminates some of the individual dependent upon probability. The fitter individuals are more likely to survive and reproduce. Survival individuals are chosen by replacement so it is possible that some individuals are chosen more than one. Possible solutions are crossed over and recombined. Mutation operator change individual values randomly. This eliminates converging solution to

certain value. Mutation is applied only to certain percentage of the total population. If percentage increases, convergence of solution gets harder, if not it eases to converge local minima. Mutation percentage is accepted as 2% of the population. The mutation provides diversity in the population. Before creating next generations, selection, crossover and mutation stages are done. In each generation, individuals' fittest values are tested, new offspring are generated and the cycle repeats.

Genetic algorithm keeps running until the same individuals start to remain without changing. This means algorithm has converged to optimum solution or solutions. The accomplishment of code is depending on criteria for success. Stopping criteria is not defined. 10 new generations are created and minimum solution has accepted as the best solution. This '10' number comes from the trial run. After that generation, the best solution among generations remains the same.

Because of general acceptance first 40 populations are randomly generated. When result of this 40-analysis is evaluated, keeping fittest points and eliminating and producing new populations phase has started. Initial population and next generations' values are given in 5.2. As it can be seen from the figure, trend is converging to optimum point. This is beneficial to reckon whole possible solution and avoid from local minima. The mean result of each generation and the best point of each generation give valuable information. If these two values are close to each other, analysis is likely to converge to optimum result. The tread line of average value of each generation is very close to the optimum solution at the last step. The ultimate point and solution of analysis are given in result part.

5.2 Analysis Model

Material properties, geometric imperfections and analysis method are same as explained at chapter 4.1, 4.2 and 4.3. Angle thickness, base thickness, bracket thickness, beam thickness and angular element height are changed throughout the optimization. As a result of this, new sections must created and angular elements' mesh must changed. Even mesh size accepted the same, element number has to be changed on angular element. Other parts element numbers remain same. The other analy-

sis' variables are same with FE model-test correlation part. By changing variables of each parameter, analysis run iteratively. As a result of each analysis, reaction force-displacement plot find out.

5.3 Results

In optimization 40 initial populations have created. Firstly, ABAQUS solve whole 40 analysis. Then MATLAB code evaluates their fittest values for each individual. Code compared the values of the maximum reaction force of each analysis. After 40 initial populations, 40 new generations are created. This process repeat 10 times. At this plot, initial population result shows between 0-1. The first-generation result is given between 1-2 and next generations keep going on. The figure 5.2 shows the whole result of optimization analysis. 440 analyses are conducted throughout the optimization process.

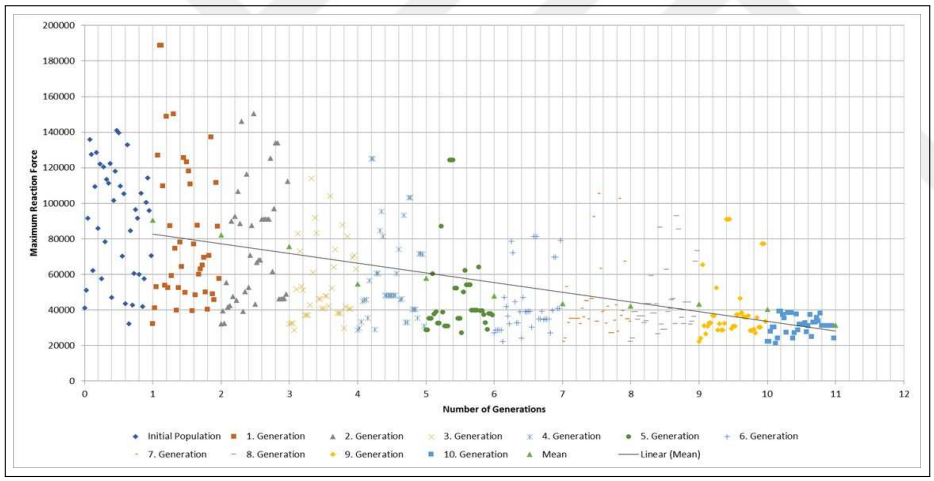

Figure 5.2: Optimization Results of Whole Analyses for Optimization - Part 1

Table 5.2: The First Part Optimum Solution(mm)

Design Parameter	Result
Angle Thickness	0.6
Angle Height	120
Base Thickness	1.42
Bracket Thickness	0.81
Beam Thickness	0.81

First buckling occurs at the beam webs. It occurs easily at 10 mm deformation without

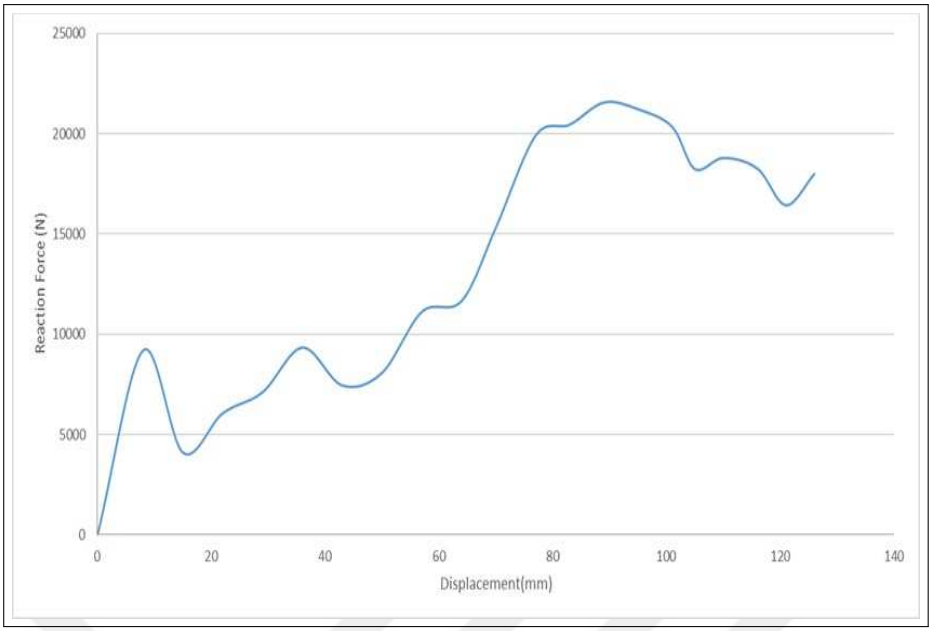

Figure 5.3: Optimum Solution Reaction Force - Displacement Curve

generating peak loads at the ground. The second buckling also occurs at low force levels at 35 mm deformation. After 70 mm deformation, angle starts to compress. Thus, peak force appears at angle buckling. Buckling of assembly has increased and got closer to each other. Initial Shape, initial buckling, peak load and final shape of the assembly are given in figures 5.4,5.5,5.6,5.7,

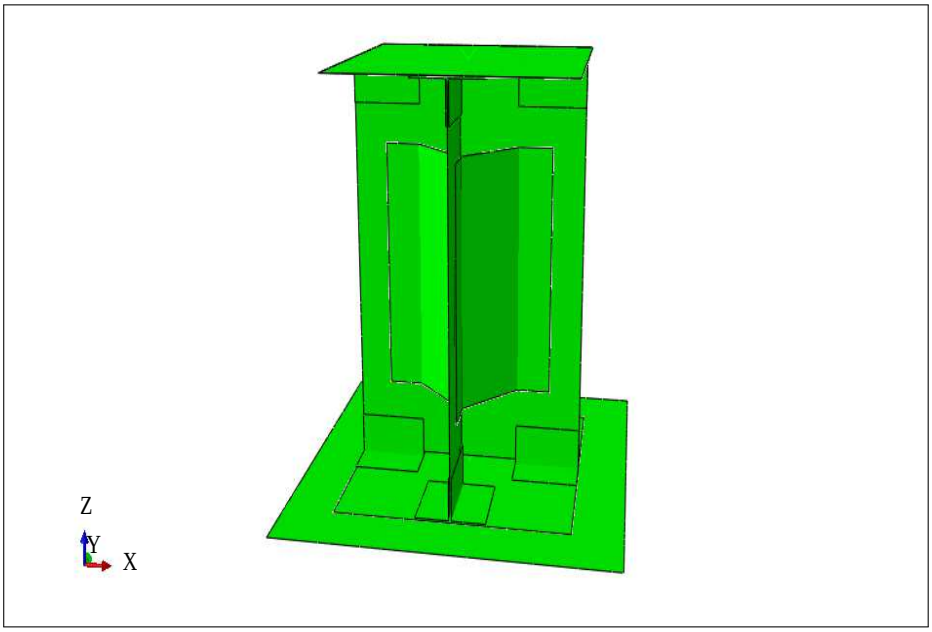

Figure 5.4: The Initial Shape of Optimum Solution(MPa)

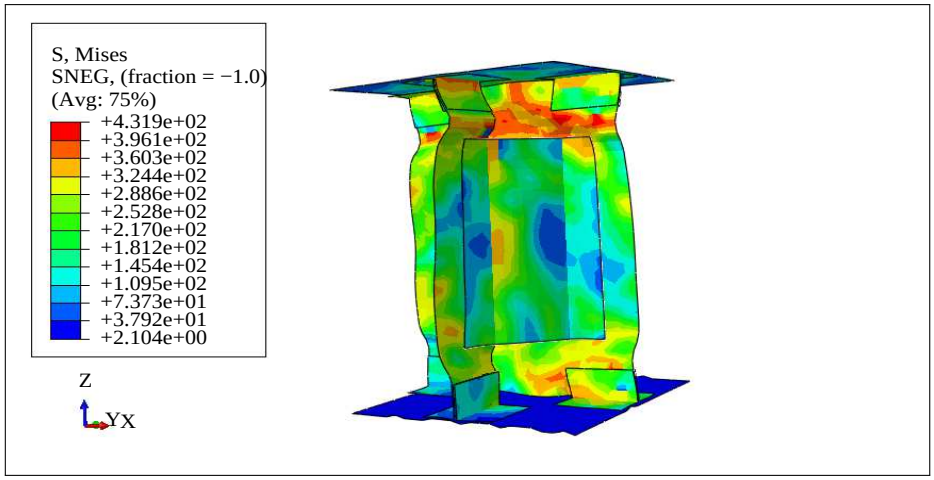

Figure 5.5: Optimum Solution Von Mises Plot at Initial Buckling(MPa)

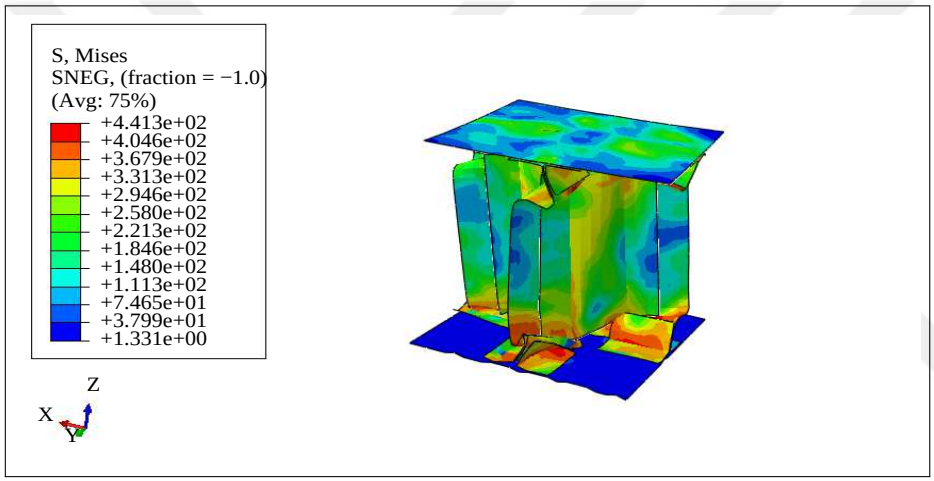

Figure 5.6: Optimum Solution Von Mises Plot at Peak Force(MPa)

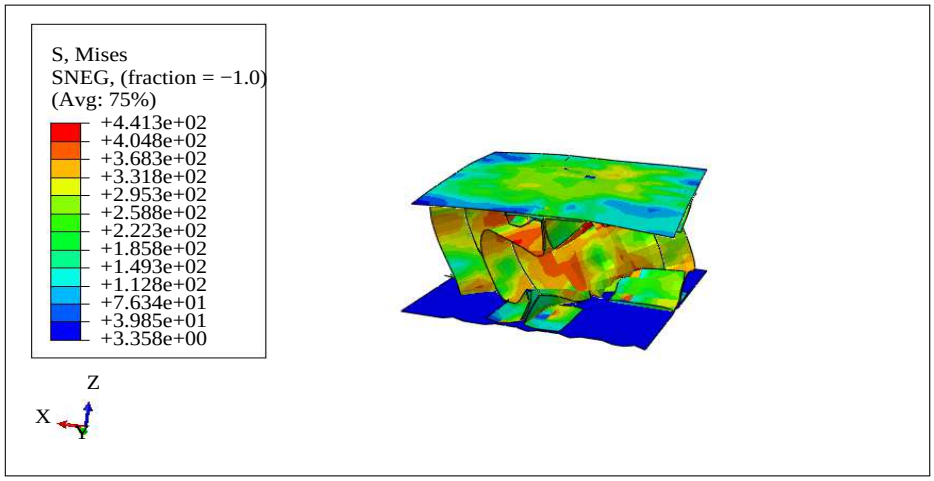

Figure 5.7: Optimum Solution Von Mises at Final Shape(MPa)

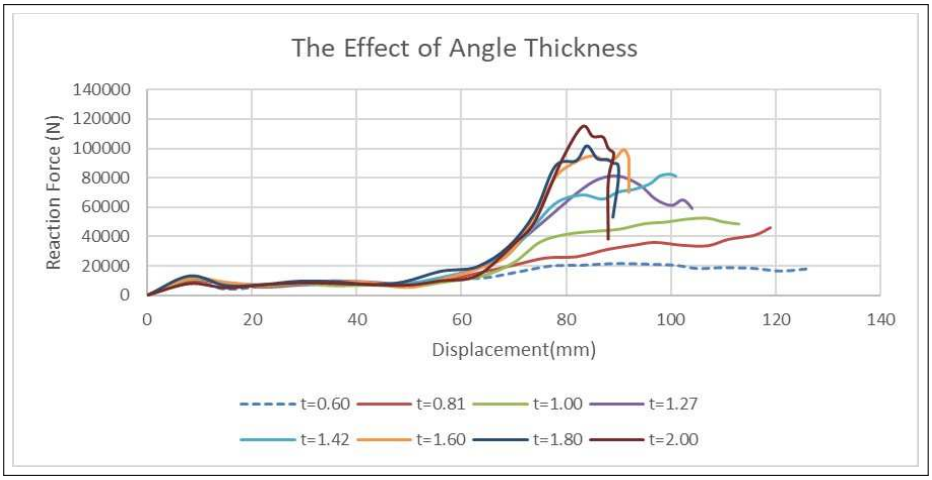

Figure 5.8: Load-Shortening Curves of Part-1 Optimum Solution over a Range of Angle Thicknesses

First, angle thickness contribution is examined. Reaction force - displacement plots are compared per variable angle thicknesses. As can be seen from plot, angle thickness has major effect on maximum RF. Maximum RF is increased with increasing thickness. Maximum RF of 2.00 mm sheet is more than 110 kN. However, maximum RF of 0.6 mm sheet thickness is 20 kN which is less than 20% of 2.00 mm sheet result. Another outcome is thinner sheet assemblies elongate longer than thicker assemblies. Section dissipates same amount of energy without increasing RF.

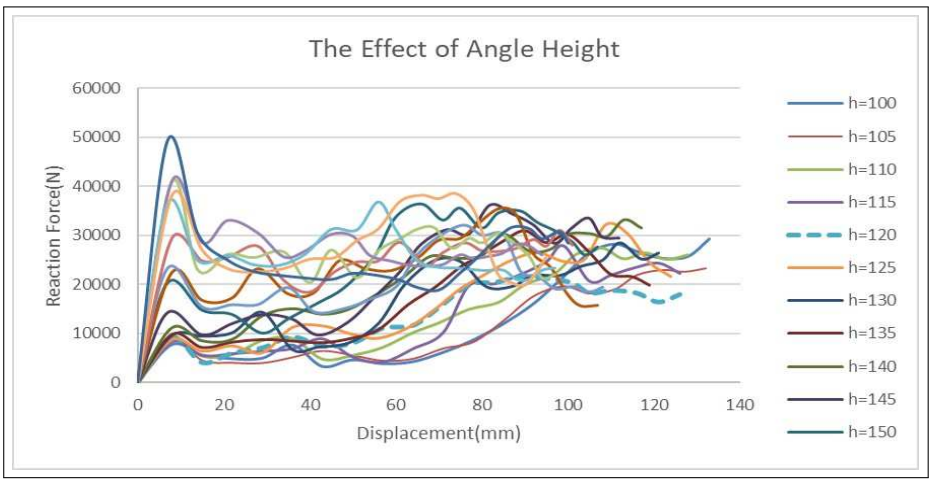

Figure 5.9: Load-Shortening Curves of Part-1 Optimum Solution over a Range of Angle Heights

The angle height also has considerable effect on optimum solution. At shorter height, there is no connection between results. However, after 160 mm height, maximum RF is increased with increasing height. Sections with higher angle deform less compared to the remaining. The reason is short angles enforce web to buckle first. Then angle is started to buckle. Even though the shorter webs are less than 100 mm, has lower RF then optimum solution, RF has started to increase dramatically at the end of the crash. Crash load compress specimen very high degrees so final buckle generates high loads. The RF is 50 kN at 190 mm, 20 kN at optimum design. The effect is not as much as the thickness of angle but it has remarkable effect on a better design.

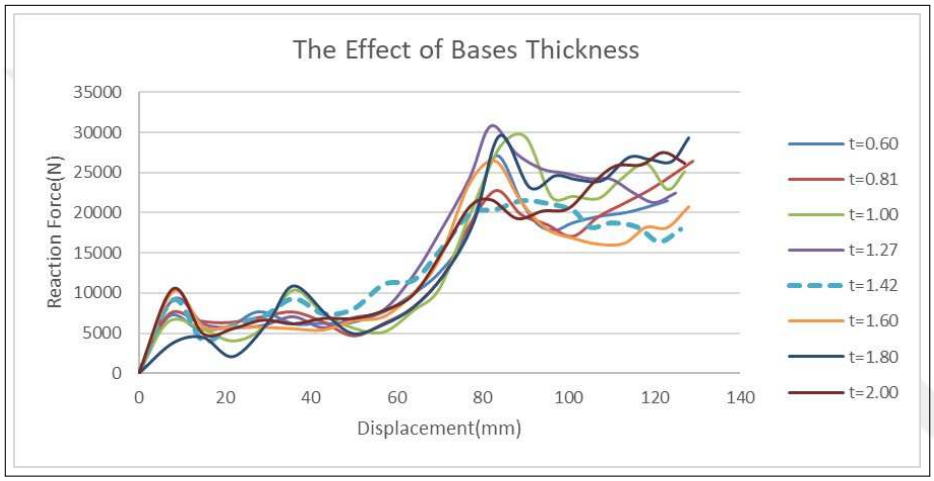

Figure 5.10: Load-Shortening Curves of Part-1 Optimum Solution over Range of Base Thicknesses

Base thickness change has limited influence on design result. Base has nearly no shape changes at the crash. Energy is dissipated by shape changes and buckling. Thus, with respect to angle variables, base thickness has a very little contribution on design.

The other parameter is the thickness of L bracket. These brackets are buckling at very last. At some scenarios, they do not buckle either. This depends on other parts heights and thicknesses. However, bracket are riveted to top and bottom part of assembly. Buckling of these parts must be occurring at last independent from their thicknesses. Thus, each variable's RF values increased with displacement. Thickness effect is

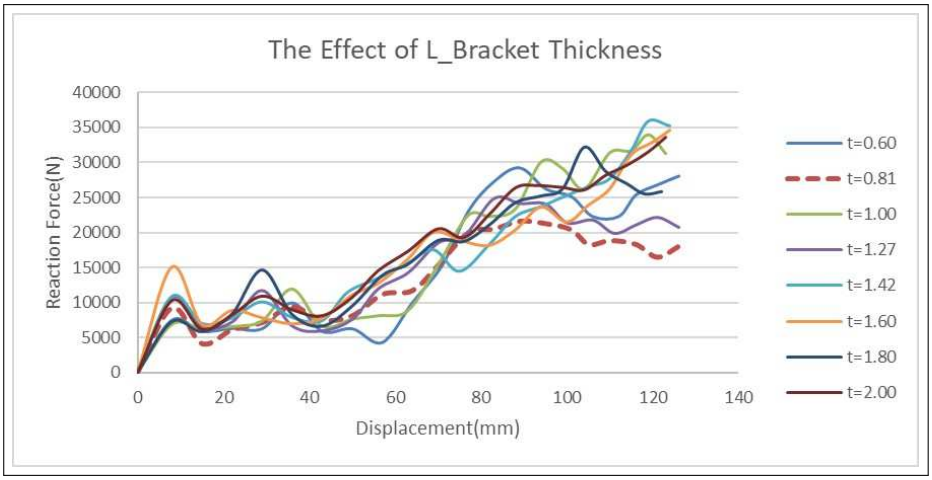

Figure 5.11: Load-Shortening Curves of Part-1 Optimum Solution over Range of Bracket Thicknesses

going similarly early 80 mm deformation. When compression is increased, effect of the bracket has appeared. The deformation values are nearly same for each thickness. The degree of influence of this variable is also limited. The ratio between maximum and minimum values is less than 1.5.

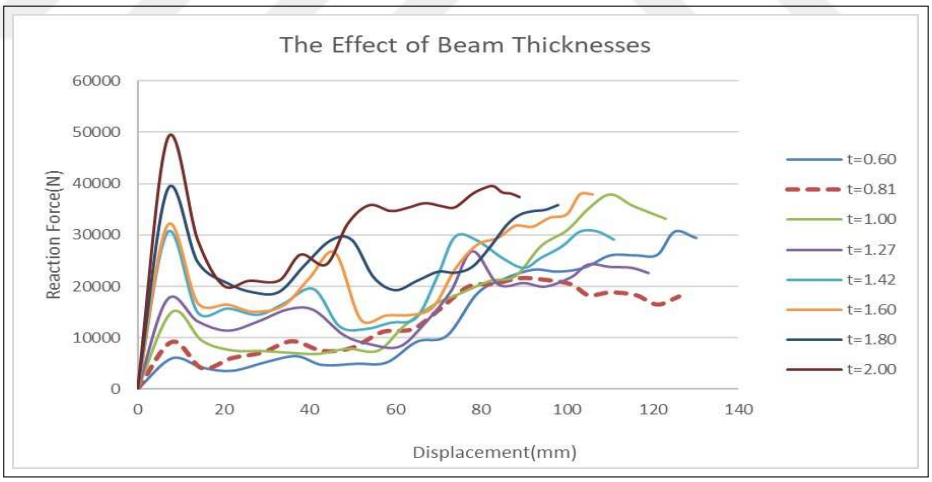

Figure 5.12: Load-Shortening Curves of Part-1 Optimum Solution over Range of Beam Thicknesses

From this plot, we can conclude that initial buckling always occurs at beams at nearly same place. Thickness of beam has direct effect on optimum solution. Thicker beam assemblies deform less than thinner sheet beams. Thinner sheet beams also deform

much more which cause high peak loads at the end of deformation. The contribution of beam thickness is very high. 2.00 mm web maximum RF is more than the double RF of 0.81 mm web. Angle and beams are two biggest vertical energy absorber elements. However, their behaviours during crash are different. Thicker beams create high peak loads at the beginning of collision. The reason is beam always buckle before angle. Stress peak values occur on beam sheets. Angle always starts to buckle after web buckling. Beam load-shortening plot is similar to angle height load-shortening plot. Higher angles curve very close to thicker beam curves. Increased stiffness in vertical direction, either by increasing thickness or adding stiffer angle, increases peak loads. Intersection elements behave like hard stiff columns.

CHAPTER 6

OPTIMIZATION - PART 2

6.1 Optimization Theory

In second optimization part, material is added as a design variable. Besides aluminium, magnesium and titanium are added. Mechanical properties of these materials are given in figures 6.2 and 6.1 Magnesium is newly used as a crash absorber material in automotive. Titanium is also over utilized as aerospace material because of lightweight and high strength. Titanium is too expensive to use for the whole structure. Magnesium strength is relatively low to use on whole subfloor structure. Thus, these materials are used only for connection elements like bracket and angular element.

Table 6.1: The Mechanical Properties of Magnesium[35]

Young Modulus	E	45 GPa
Yield Stress	σ_y	151 MPa
Yield Strain	ϵ	0.016
Poisson's Ratio	ν	0.35

Table 6.2: The Mechanical Properties of Titanium[35]

Young Modulus	E	110 GPa
Yield Stress	σ_y	900 MPa
Yield Strain	ϵ	0.07
Poisson's Ratio	ν	0.31

Design variables have become angular element thickness, angular element height, beam thickness, bracket thickness and base thickness and material. To optimize these variables MATLAB Optimtool is used same as the first part. Because of Optimtool

integer input values, material array is also used to create input file. Array for design variables are given below,

MATLAB generates six integer numbers for six design variables, then input values are copied to python file as an ABAQUS input. After analysis is finished, maximum value of reaction force-displacement curve is copied to MATLAB. Then, new generations are created and same procedure repeated. The remaining optimization theory is same as explained in Chapter 5.1.

Table 6.3: Domain of the Variables (Optimization Part 2)

Variables	Variable Domain
Thickness	0.6 0.81 1 1.27 1.42 1.6 1.8 2
Height	100 105 110 120 ..... 185 190
Material	Aluminium Titanium Magnesium

Analysis is concluded at 10th Generations. This '10' number comes from trial run. After that generation, the best solution among generations remains same. At this part to enlarge seek area, more initial individuals are generated. 80 initial population are generated which means total 880 analysis run because possible solution domain increased 3 times. 880 analysis results are given in Figure 6.13.

6.2 Analysis Model

Since new materials are added, plasticity of the new materials should be defined same as aluminium. New design materials are magnesium and titanium. Stress-strain curves of materials are given in Figure 6.1 - Magnesium Stress-Strain Curve (Group 6) and Figure 6.1 - Titanium Stress-Strain Curve. Analysis method is the same with first optimization part. Beside this, sections have created with new property before assigned on parts.

In this design method, connector element like angle and brackets can be produced from magnesium or titanium which is a 6th. Properties of magnesium and titanium are given in figure 6.1 and 6.2. Titanium and aluminium is used for connector elements because titanium and magnesium are used as crash absorber elements in in-

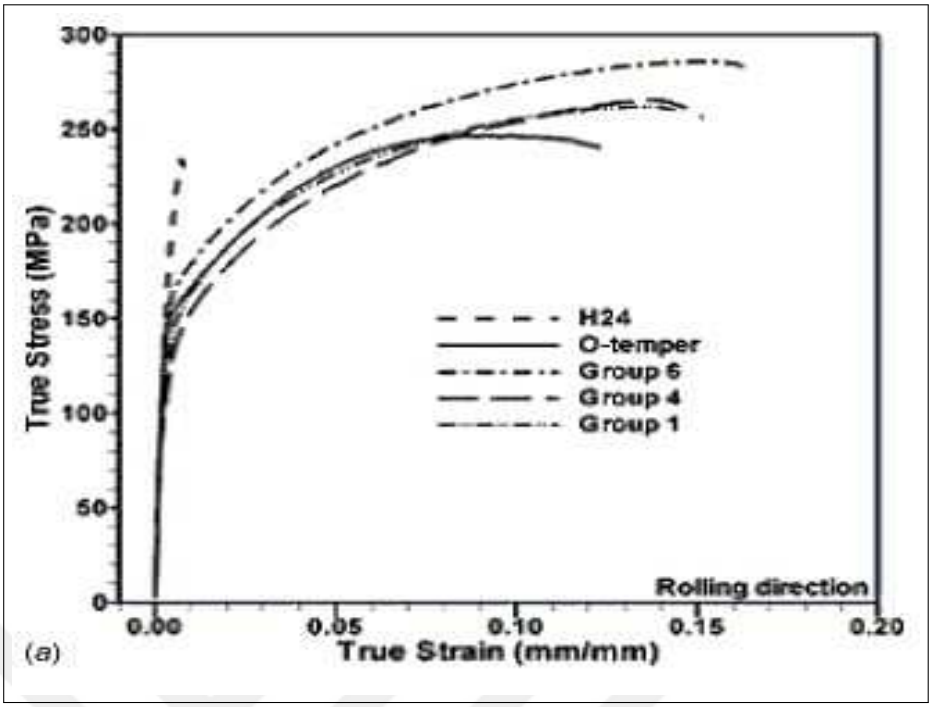

Figure 6.1: Magnesium Stress-Strain Curve (Group 6)

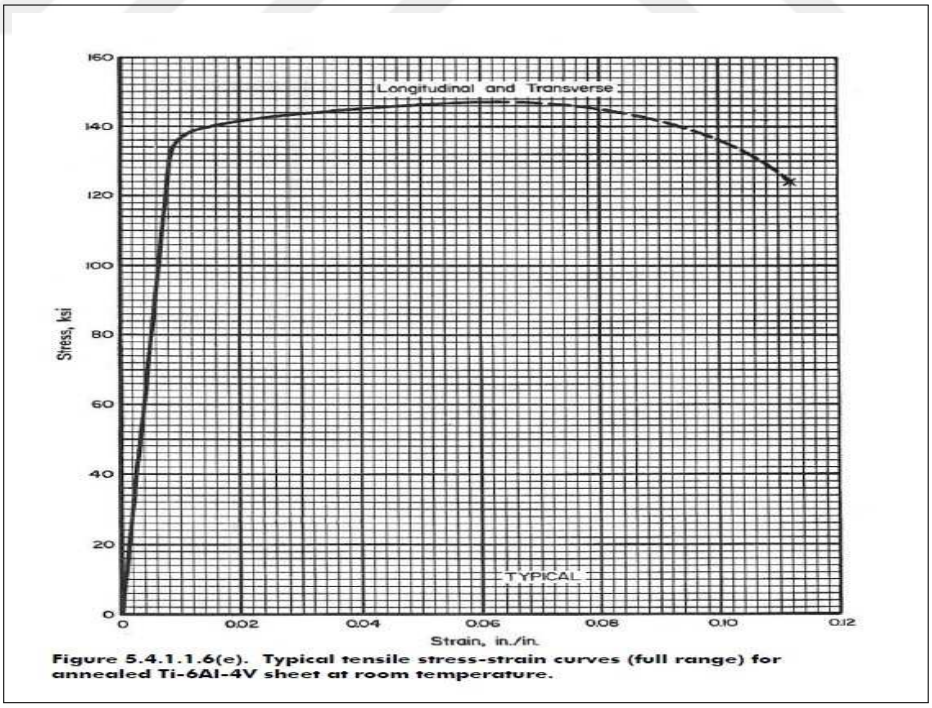

Figure 6.2: Titanium Stress-Strain Curve

dustry. Beams, frames and bases are preferred as aluminium because these are very big parts. In model, only a part of them is used. It is not feasible to use crash absorber material for the whole structure. These materials are very expensive to use in excessive amount.

6.3 Result

In this optimization, 80 initial populations have created. It is developed up to 10 generations. 880 analysis have conducted to find optimum solution among 233 472 possible solutions. In part 1, 440 analyses have run which is less than half of the second part. In second part, total analysis number has increased to get a more closer result.

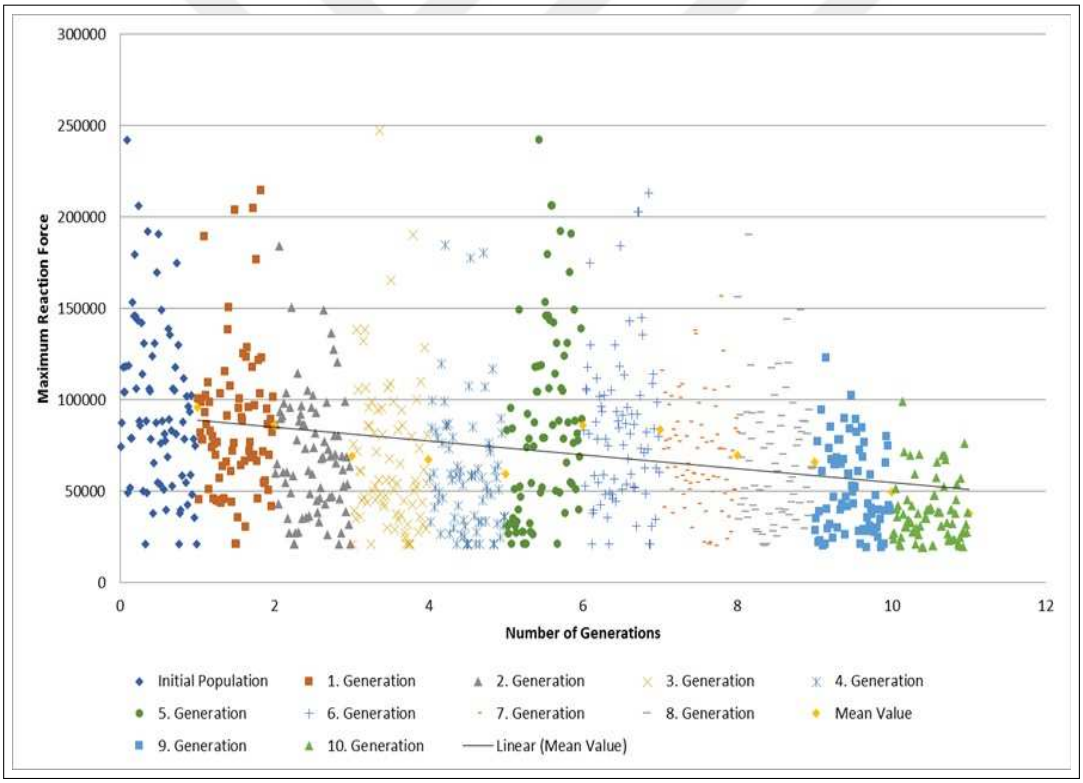

Figure 6.3: Optimization Results of Whole Analyses for Optimization - Part 2

The optimum parameters and maximum reaction force of analysis are found as 6.4. Magnesium is better material option. The optimum result is found as 19.3 kN. This result is 10% less than first optimization part.

Table 6.4: The First Part Optimum Solution

Design Parameter	Result
Angle Thickness	0.6 mm
Angle Height	120 mm
Base Thickness	1.42 mm
Bracket Thickness	0.81 mm
Beam Thickness	0.81 mm
Material	Magnesium
Maximum RF	19.3 kN

The maximum reaction force is taken from RF-Displacement curve. Maximum force of the RF-displacement curve is aimed to minimize. The result of second part is given is 6.4,

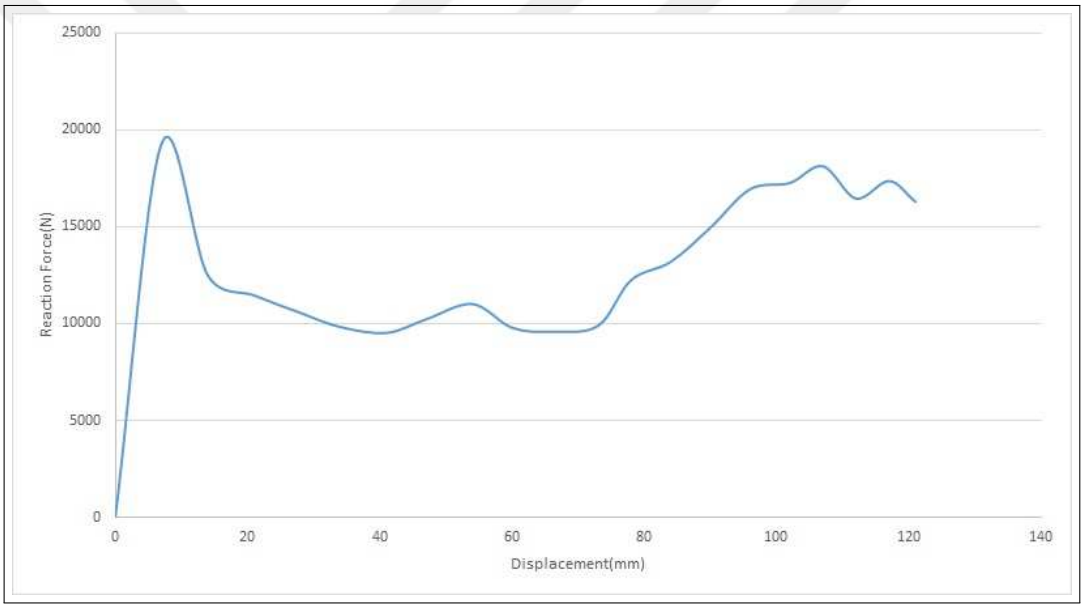

Figure 6.4: Optimum Solution Reaction Force - Displacement Curve for Part 2

As s result of this optimization process, optimum solution has found different than part 1 result. Part 1 maximum reaction force is found as 21556 N. Material variable improve reaction force to 19299 N which is 11.7% less than first result. Even two assemblies are 110g, by changing material, maximum reaction force decrease more than 10% without increasing weight.

Optimum solution, the deformation at initial buckling, the deformation at peak load and final deformation figures are given in figures 6.56.66.76.8.

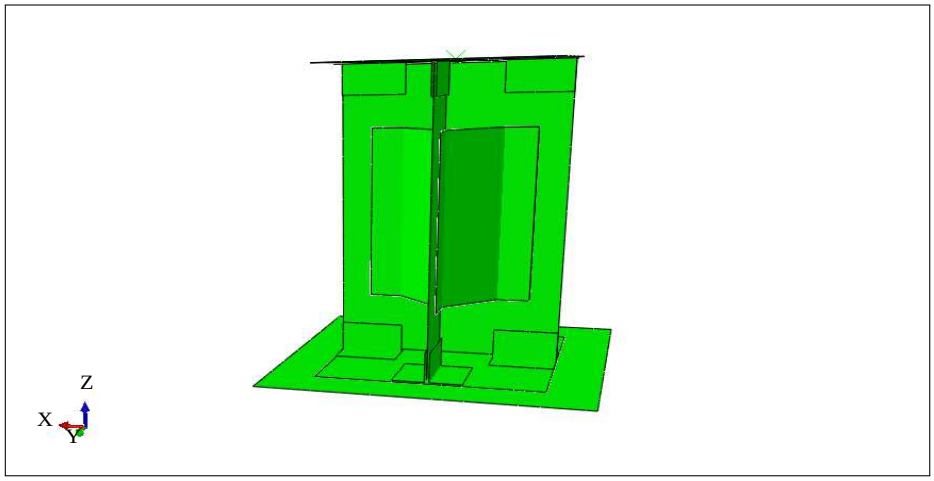

Figure 6.5: The Initial Shape of Part 2 Optimum Solution

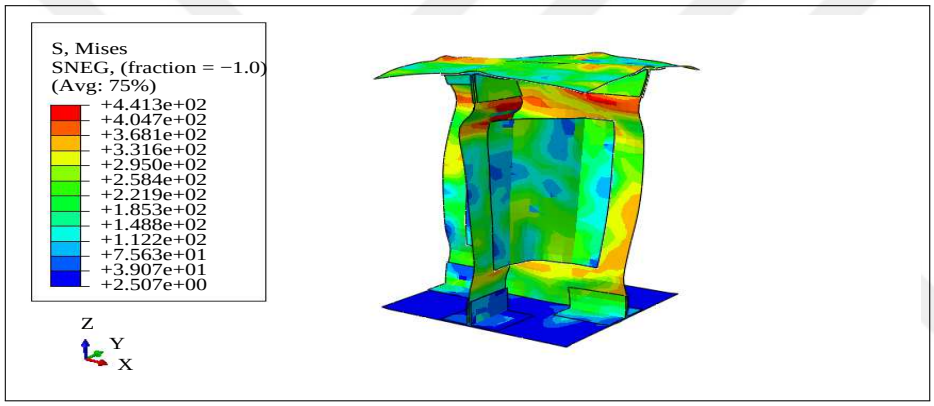

Figure 6.6: Part 2 Optimum Solution Von Mises Plot at Initial Buckling(MPa)

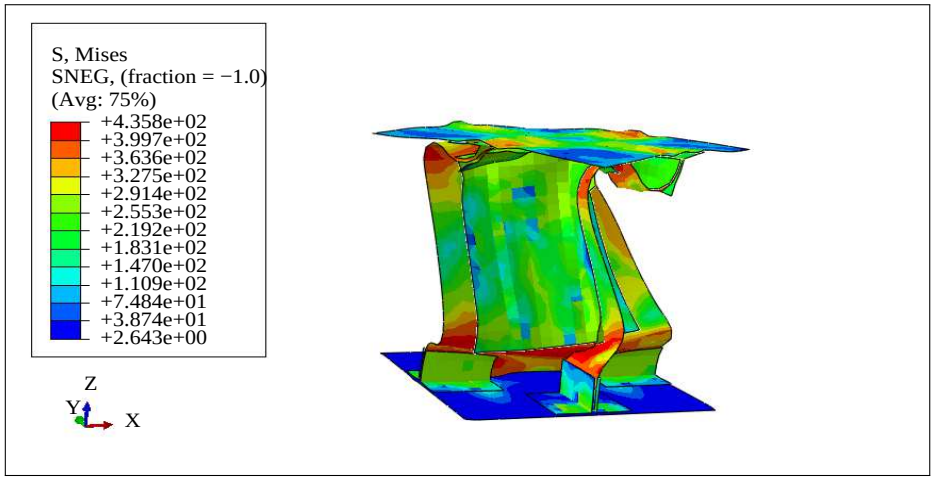

Figure 6.7: Part 2 Optimum Solution Von Mises Plot at Peak Force(MPa)

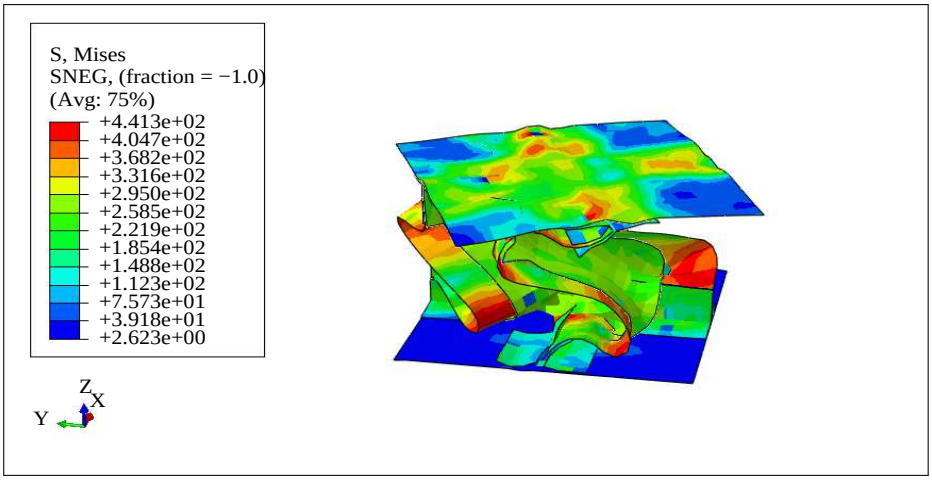

Figure 6.8: Part 2 Optimum Solution Von Mises at Final Shape(MPa)

After that point, contribution of each parameters are detailed. For one parameter, all possible solutions in design domain are analysed and remaining parameters kept constant. For each design parameter, the effect of different design input on maximum reaction force is compared. The remaining design parameters are kept as found in the best solution.

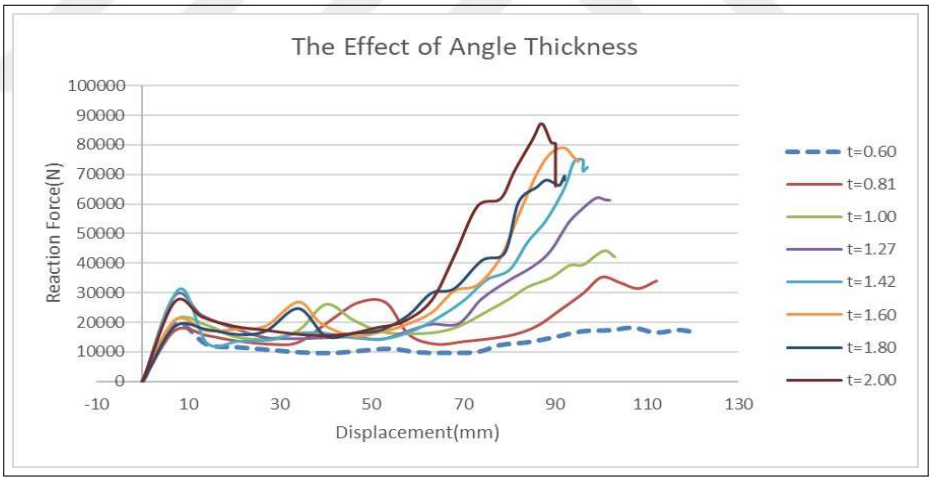

Figure 6.9: Load-Shortening Curves of Part-2 Optimum Solution over Range of Angle Thicknesses

Initial reaction force of each thickness is close to each other. The reason is initial buckling starts from beam webs. After 70 mm deformation angle starts to compress and stress developed. Amount of elongation and peak stress are strongly related with angle thickness. Compared to first part results, magnesium connector elements de-

crease maximum reaction force 20-30 % for some sections. The other outcome is that, assemblies with magnesium bracket and angle elongate less than aluminium results. This probably relates with that magnesium angle buckling is easier than aluminium so it dissipates crash energy with less deformation.

Table 6.5: Reaction Force Comparison of Part 1 and Part 2 over Range of Angle Thicknesses

Angle thickness	Part-1, Maximum Reaction Force Value	Part-2, Maximum Reaction Force Value
0.6	21556	19299
0.81	46110	35146
1	52438	44272
1.27	80980	62047
1.42	82427	74955
1.6	99092	79027
1.8	101774	69535
2	114508	87117

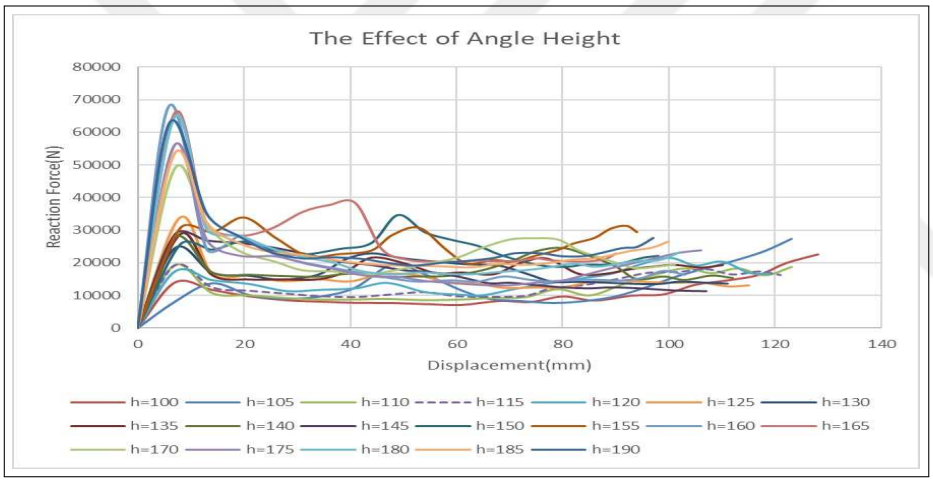

Figure 6.10: Load-Shortening Curves of Part-2 Optimum Solution over Range of Angle Height

Angle height change shows similar effect with part 1. Shorter angles create less load however higher angles create high peak loads. After 165 mm height, there is a great jump at the peak loads. Higher angles hold firm beams and obstruct buckling. It jumps to 1.5 times of high peak load of 160 mm angle height. Since optimum solution beam thicknesses are 0.6 mm thicker than first part, vertical section stiffness advance first part. High peak loads are closely related with vertical stiffness. That's why second part peak loads are much higher than first part. Elongation is same with angle which is shorter than the first part. The main energy absorber parts are beams. While beams

get thicker, compression of beams get harder. Thus, assembly deforms less.

Table 6.6: Reaction Force Comparison of Part 1 and Part 2 over Range of Angle Height

Angle Height	Part-1, Maximum Reaction Force Value	Part-2, Maximum Reaction Force Value
100	29314	22584
105	23362	27435
110	27364	19360
115	27959	19299
120	21556	21447
125	32206	33870
130	28520	24575
135	31024	28800
140	33130	27864
145	36274	28794
150	36413	34658
155	35497	33966
160	32105	68243
165	31128	65873
170	40852	49046
175	41112	56255
180	36867	64688
185	38541	53576
190	49372	62948

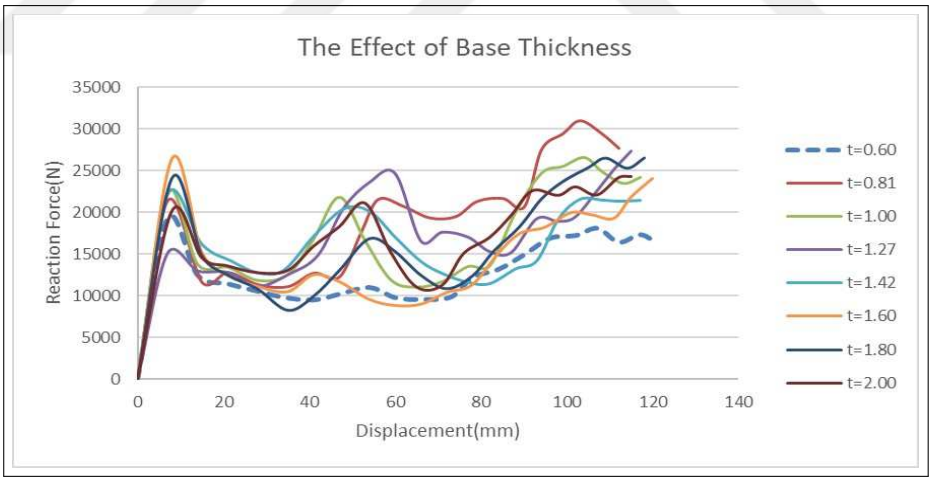

Figure 6.11: Load-Shortening Curves of Part-2 Optimum Solution over Range of Base Thicknesses

Peak load contribution of base thickness change is the same. Since part is perpendicular to crash direction, its contribution is also very limited. The assembly thickness and sections have changed so maximum load point has shifted to the beginning. In early crash, thickness contribution goes in order. After 40 mm deformation, disassociation

has started. Each thickness contribution becomes clear.

Table 6.7: Reaction Force Comparison of Part 1 and Part 2 over Range of Base Thicknesses

Base thickness	Part-1, Maximum Reaction Force Value	Part-2, Maximum Reaction Force Value
0.6	27041	19299
0.81	26441	31026
1	29477	26572
1.27	30799	27320
1.42	21556	22204
1.6	26478	26456
1.8	29557	26509
2	27471	24310

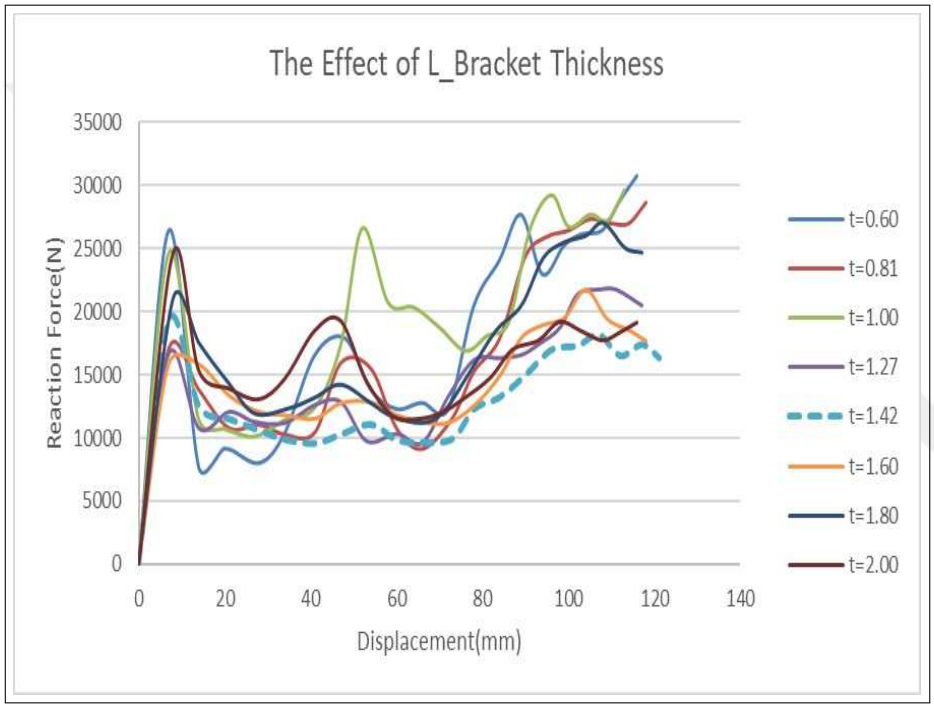

Figure 6.12: Load-Shortening Curves of Part-2 Optimum Solution over Range of Bracket Thicknesses

Same with bases, contribution of the bracket on reaction force is limited. After 40 mm deformation, the effect of each thickness differs from each other. Even base thickness change contribution on total dissipation is very small, all thickness contribution is very different from each other. 1.00 mm thickness bracket goes different from other thickness; it buckles very around 55 mm deformation. The remaining specimens are buckling at last, where whole structure collapses. Because of this, effect on dissipation is negligible. Structure dissipates nearly whole energy before bases buckle.

Table 6.8: Reaction Force Comparison of Part 1 and Part 2 over Range of Bracket Thicknesses

Bracket thickness	Part-1, Maximum Reaction Force Value	Part-2, Maximum Reaction Force Value
0.6	29163	30725
0.81	21556	28678
1	33962	29637
1.27	24910	21800
1.42	35918	19299
1.6	34574	21720
1.8	32204	27026
2	33624	24597

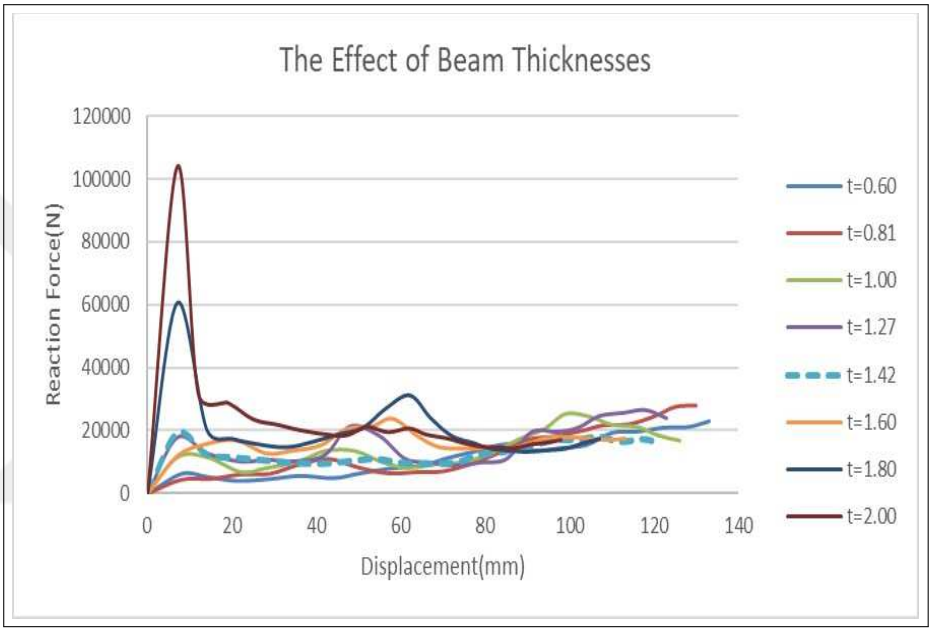

Figure 6.13: Load-Shortening Curves of Part-2 Optimum Solution over Range of Beam Thicknesses

When angle parts produced from weaker materials, beams start to dissipate much more energy than before. Thus, thickness contribution can reach enormous levels. For 2.00 mm beam thickness, second part maximum reaction force is doubled. There is also jump between top two thickness and remaining ones. After the peak load at the beginning, forces decrease because much of the energy is dissipated. Compression amount is also directly related with beam thicknesses. Different than part 1, load-shortening curves go similar with changing thickness after 30 mm deformation. When whole assembly is produced from aluminium, the results are diverse from each other at the end of crush.

Table 6.9: Reaction Force Comparison of Part 1 and Part 2 over Range of Beam Thicknesses

Beam thickness	Part-1, Maximum Reaction Force Value	Part-2, Maximum Reaction Force Value
0.6	30617	23058
0.81	21556	27855
1	37934	25219
1.27	26805	26423
1.42	30666	19299
1.6	37891	23824
1.8	38822	60363
2	48844	103964

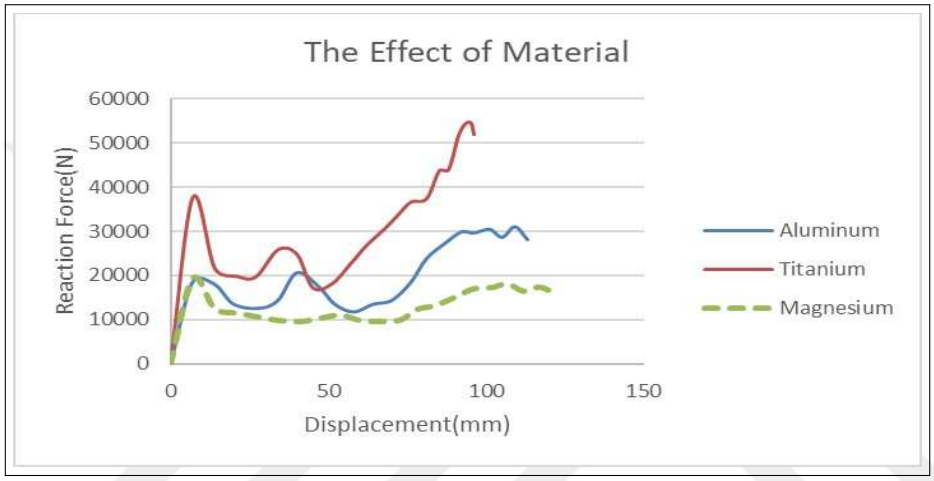

Figure 6.14: Load-Shortening Curves of Part-2 Optimum Solution over Range of Material Type

Table 6.10: Maximum Reaction Force Result over Range of Material Types

Material	Part-2, Maximum Reaction Force Value
Aluminum	30957
Titanium	54619
Magnesium	19299

The main aim to conduct second run is to evaluate material effect on energy absorption. Material plays critical role on energy dissipation. For material comparison, all other parameters keep constant, only material of the parts has changed. The given results on figure 6.14 is applicable for the optimum solution. There are other solutions with titanium parts better than results are given in table 6.5. However the effect of material on the optimum solution is compared. At the beginning aluminium and magnesium show similar initial buckling. Titanium shows different initial buckling load

than others because its yield stress is much higher than magnesium and aluminium. Since angle and bracket start to compress at the end, their contribution can be seen clearly. Total deformation is strongly related with material yield stress. That's why ductile material elongates longer.

CHAPTER 7

DISCUSSION AND CONCLUSION

This thesis is about the optimization of helicopter subfloor structural element. The main aim is to determine lightweight and energy absorber floor structure. Contribution of each part and material effect is investigated. To do this optimization, ABAQUS is used as finite element program and MATLAB is used as optimization solver.

Analysis model is correlated with test result[10]. In paper, finite element model and test results are compared. To create realistic analysis model, FE results and test result must be correlated. In crash test, high peak loads are the most important result data. Model and test are correlated very well at high peak loads. After initial buckling test loads are lower than model result. This is related to imperfections that cannot be incorporated to the FE model. The deformation pattern is also very similar to the test. This is also supports that imperfections could decrease load after initial buckling. It is considered that required data is good correlated between test and result.

In elastic region, both paper's numerical result and ABAQUS result loads are higher than test result. This is probably related with mesh type. 4 node shell elements are poor in bending. That's why elastic region difference could occur.

Material load carrying capacity increases linearly until it buckles. From that point, plastic deformation has started. Load carrying capacity of the specimen decreases. At first buckling, local region keep deforming plastically, neighbour elements stiffness has increased. Then another localized buckling occurs again. The following buckling cannot reach the same amount of force as before, because initial buckling creates imperfection on assembly. This is valid until first couple buckling then load - shortening gradient start to increase. The reason is that assembly compressed so much, any fur-

ther deformation and increments need larger loads than before. Specimen cannot be crushed to zero length, thus at some point, stiffness of the deformed specimen goes infinity.

After initial buckling, specimen goes in plastic deformation. If specimen deformation is limited, the highest load occurs here. It cannot reach pre-buckling forces because initial buckling creates imperfection. If buckling keeps continuing and deformation passes the critical level, stiffness and force will increase. After the edges of the specimen buckle, stiffness at the specimen's center has increased. Stress starts to develop at the center of the specimen. Buckled edges are no longer supporting the peak load.

Each parameter are compared with other possible solutions results. For each parameters, different inputs are applied while other parameters were constant. The effect of each parameters on maximum reaction force are examined separately. As a result of this comparisons, the effect of bases and bracket have little effect on energy absorption capability. Parts with vertical height have principal effect on deformation, buckling and energy dissipation. Stiffness of assembly has increased with increasing parts' vertical dimension such as beam, frame and angle. Angle height has a critical effect on energy absorption. Generally, assemblies with shorter angle have better energy absorber specimens. There is also a high jump after 170 mm. When angle height passes this value, peak loads nearly doubled compared to 165 mm height angle. The best solution is found by optimizing their contribution either less or more.

The peak load of initial model result is found as 53.3 kN. In the first optimization part, the maximum reaction force of specimen decreased to 21.5 kN. This is 40% less than initial model. For further decrease on the maximum reaction force, material is added as another design variable. Material has critical effect on energy absorption. Even weight of the specimen remains same, more crashworthy solution has designed. With material, peak load has decreased up to 10% more compared to aluminium structure. It is found that by implementing another material into junction element, peak loads can decrease.

The results obtained in this study show that energy dissipation capacity of the helicopter subfloor intersection element can be improved by modifying junction element thickness, shape and material. Even it is impossible to make the test of hundreds of

specimens, it can be optimized in finite element programs. The results of the finite element program do not perfectly match to the test results but it will be better in the future.

Accuracy and performance of the structure could increase with further investigations. To lookout for future works can be summarized as follows,

- Subfloor intersection element is optimized under crash loading. The primary function of the structure is to carry flight loads. To get more applicable result, flight loads should include optimization. The structure, which only good at energy dissipation cannot used on flying helicopter.
- Magnesium and titanium is used other than aluminium. New materials could be added to get better result like composites.
- New coupon tests with other materials will increase the correlation between test model and finite element model.

REFERENCES

[1] Shanahan, D. F. Basic principles of helicopter crashworthiness. *Fort Rucker, Ala.: U.S. Army Aeromedical Research Laboratory.*, 1993.

[2] Karagiozova, D., and Jones, N. Dynamic effects on buckling and energy absorption of cylindrical shells under axial impact. *Thin-Walled Structures*, 39(7), 583-610, 2001.

[3] Lanzi, L., Airoldi, A., Astori, P., and Grassi, F. (n.d.). Optimisation of energy absorbing subsystems for helicopter vertical crashes.

[4] Song, J., Zhou, Y., and Guo, F. A relationship between progressive collapse and initial buckling for tubular structures under axial loading. *International Journal of Mechanical Sciences*, 75, 200-211, 2013

[5] Fyllingen, Ø, Langmoen, E., Langseth, M., and Hopperstad, O. Transition from progressive buckling to global bending of square aluminium tubes. *International Journal of Impact Engineering*, 48, 24-32, 2012.

[6] K.E. Jackson, E.L. Fasanella. Crash Certification by Analysis - Are We There Yet?. *US Army Research Laboratory; K.H. Lyle, NASA Langley Research Center*

[7] Shpji, H., Miyaki, H., and Matsumoto, H. Full-Scale crash test of a civil helicopter at JAXA

[8] Certification Specifications for Large Rotorcraft CS - 29 Amendment 2. *European Aviation Safety Agency Specifications*, 2008.

[9] Kindervater, C. M. Aircraft and Helicopter Crashworthiness: Design and Simulation. *Crashworthiness of Transportation Systems: Structural Impact and Occupant Protection*, 525-577, 1997.

[10] Bisagni, C. Crashworthiness of helicopter subfloor structural components. *International Journal of Impact Engineering*

[11] Qiao, J., Chen, J., and Che, H. Crashworthiness assessment of square aluminum extrusions considering the damage evolution *Thin-Walled Structures*, 44(6), 692-700, 2006.

[12] Anghileri, M., Milanese, A., and Surini, A. Optimization of helicopter subfloor components under crashworthiness requirements. 2001.

[13] Maia, L. G., and Paulo Henriques Iscold Andrade De Oliveira A Review of Finite Element Simulation of Aircraft Crashworthiness. *SAE Technical Paper Series.*, 2005.

[14] Guida, M., and Marulo, F. Partial Modeling of Aircraft Fuselage During an Emergency Crash Landing. *Procedia Engineering.*, 88, 26-33, 2014.

[15] Hughes, K., Vignjevic, R., and Campbell, J. Experimental observations of an 8 m/s drop test of a metallic helicopter underfloor structure onto a hard surface: Part 1. *Proceedings of the Institution of Mechanical Engineers, Part G: Journal of Aerospace Engineering*, 221(5), 661-678, 2007.

[16] Atkinson, A. C., and Donev, A. N. The Construction of Exact D-Optimum Experimental Designs with Application to Blocking Response Surface Designs. *Biometrika*, 76(3), 515, 1989.

[17] Annett, M., and Horta, L. Comparison of Test and Finite Element Analysis for Two Full-Scale Helicopter Crash Tests. *52nd AIAA/ASME/ASCE/AHS/ASC Structures, Structural Dynamics and Materials Conference*, 2011.

[18] Langseth, M., Hopperstad, O., and Hanssen, A. Crash behaviour of thin-walled aluminium members. *Thin-Walled Structures*, 32(1-3), 127-150, 1998.

[19] Kim, D., Lee, S., and Rhee, M. Dynamic crashing and impact energy absorption of extruded aluminum square tubes. *Materials & Design*, 19(4), 179-185, 1998.

[20] Langseth, M., Hopperstad, O., and Berstad, T. Crashworthiness of aluminium extrusions: Validation of numerical simulation, effect of mass ratio and impact velocity. *International Journal of Impact Engineering*, 22(9-10), 829-854, 1999.

[21] Ramakrishna, S., and Hamada, H. Energy Absorption Characteristics of Crashworthy Structural Composite Materials. *KEM Key Engineering Materials*, 141-143.585, 1998.

[22] Harrigan, J., Reid, S., and Peng, C. Inertia effects in impact energy absorbing materials and structures. *International Journal of Impact Engineering*, 22(9-10), 955-979., 1999.

[23] Deletombe, E., Delsart, D., Kohngrüber, D., and Johnson, A. F. Improvement of numerical methods for crach analysis in future composite aircraft design. . *Aerospace Science and Technology*, 4(3), 2000.

[24] Albertini, C. Labibes, K. and Solomos, G. Calibration of impact rigs/crashworthiness testing of thin metal boxes. 2003.

[25] Lyle, K. H., Bark, L. W., and Jackson, K. E. Evaluation of Test/Analysis Correlation Methods for Crash Applications. *Journal of the American Helicopter Society*, 47(4), 233, 2002.

[26] Fasanella, E. L., Jackson, K. E., and Lyle, K. H. Finite Element Simulation of a Full-Scale Crash Test of a Composite Helicopter. *Journal of the American Helicopter Society*, 47(3), 156-168, 2002.

[27] Jones, N. (n.d.) Analysis and Design of Flight Vehicle Structures. *Philadelphiea: G.W. Jacobs*, 1973.

[28] Amdahl, J., Mohammed, A. K., and Skallerund, B. (n.d) Collapse analysis of stiffened panels during accidental conditions.

[29] Sivanandam, S., and Deepa, S. (n.d.) Genetic Algorithm Optimization Problems. *Introduction to Genetic Algorithms*, 165-209.

[30] Hegadekatte, V., Shi, Y., and Nardini, D. Buckling of Aluminium Sheet Components. *ICAA13: 13th International Conference on Aluminum Alloys 13th International Conference on Aluminum Alloys*, 897-902, 2012.

[31] R., Pifko, Winter, A., and Cronkhite, J. Crash simulation of composite and aluminum helicopter fuselages using a finite-element program. *20th Structures, Structural Dynamics, and Materials Conference*, 1979.

[32] Car, J. (n.d.). An Introduction to Genetic Algorithm. 2014

[33] Goldberg, D. E. Genetic algorithms in search, optimization, and machine learning.. *Boston: Addison-Wesley.*, 2012.

[34] Cook, R. D. Concepts and applications of finite element analysis. *India: John Wiley & Sons (Asia)*, 2003.

[35] MMPDS-08: metallic material properties development and standardization(MMPDS). *Washington, D.C: Federal Aviation Administration*, 2013.

APPENDIX A

APPENDIX NAME

A.1 First Part Optimization Result

Part 1 Optimization Inputs and Results

For Thicknesses [1 2 3 4 5 6 7 8] = [0.60 0.81 1.00 1.27 1.42 1.60 1.80 2.00]

For Height [1 2 3 4 5 6 7 8 9 10 11 12 13 14 15 16 17 18 19] = [100 105 110 . . . 185 190]

Array needs to define for optimization because code work with integer values. Outputs are given integer as well. Optimization starts with initial individuals and new generation is created at the end of each population. Outputs of optimization is given below,

Table A.1: First Part Optimization Results

Initial Points					
Angle Thk	Angle Ht	Base Thk	Bracket Thk	Beam Thk	Maximum RF
2	10	4	8	2	41212
2	9	6	1	8	51047
4	12	6	3	7	91721
7	14	3	2	6	135734
8	14	4	6	1	127523
3	5	2	5	2	62261
7	13	1	7	4	109368
7	12	5	2	7	128650
5	3	7	2	1	86024
7	4	8	2	1	122041

Continued on next page

Table A.1 – continued from previous page

Angle Thk	Angle Ht	Base Thk	Bracket Thk	Beam Thk	Maximum RF
2	10	1	1	3	57572
3	19	5	8	5	120353
7	7	5	5	7	78275
6	12	1	5	6	113577
8	6	3	3	4	111230
5	15	3	6	5	122307
2	6	7	6	4	47138
6	10	4	3	6	101479
7	14	5	5	2	117959
5	18	2	3	6	140908
6	19	6	2	2	139542
7	11	3	3	4	109735
3	3	6	1	5	70350
5	3	6	3	6	105375
2	6	6	3	2	43605
5	16	4	4	7	132925
1	5	1	1	6	32332
3	16	2	8	4	84714
1	6	8	7	5	42782
1	18	3	5	5	60551
7	7	6	5	3	96473
5	5	5	4	4	91470
3	5	8	7	5	60002
8	12	1	3	6	105609
1	10	4	1	7	41974
4	7	2	6	6	57533
4	16	7	4	3	100594
7	12	2	2	7	114152
6	10	6	3	4	96028
2	17	7	1	4	70437

1. Generations

Angle Thk	Angle Ht	Base Thk	Bracket Thk	Beam Thk	Maximum RF
1	5	1	1	6	32332

Continued on next page

Table A.1 – continued from previous page

Angle Thk	Angle Ht	Base Thk	Bracket Thk	Beam Thk	Maximum RF
2	10	4	8	2	41212
3	12	1	6	1	53013
7	13	3	6	5	127042
8	13	7	6	8	188668
7	7	6	5	6	188668
7	11	3	3	4	109735
3	5	3	6	4	53919
8	12	5	2	4	148796
2	16	6	4	2	52416
5	10	3	4	6	87350
2	12	8	5	5	59197
4	17	5	5	5	150081
4	6	7	5	1	74703
1	6	6	4	6	39774
3	9	6	7	3	52492
2	5	2	3	7	77989
5	6	5	4	7	64352
4	17	2	4	4	125538
2	5	7	4	5	49887
3	15	8	7	6	123208
4	16	7	3	6	118178
7	5	3	5	3	110631
2	10	2	3	2	39593
3	11	3	7	5	77057
2	8	2	8	3	48427
4	8	1	4	7	87446
3	1	7	6	3	60040
3	9	3	3	6	62978
3	10	4	2	7	65118
4	6	8	3	8	69572
2	11	2	4	1	49908
1	6	8	8	5	40296
4	5	8	7	6	70550

Continued on next page

Table A.1 – continued from previous page

Angle Thk	Angle Ht	Base Thk	Bracket Thk	Beam Thk	Maximum RF
2	19	2	8	8	137267
2	2	8	8	8	48918
1	16	3	1	3	45627
7	8	4	3	6	111479
5	5	7	3	2	86907
2	10	1	1	3	57572
2. Generations					
Angle Thk	Angle Ht	Base Thk	Bracket Thk	Beam Thk	Maximum RF
1	5	1	1	6	32332
2	10	2	3	2	39593
1	9	7	3	2	32385
1	18	4	5	4	55345
2	11	2	3	3	41683
2	4	1	3	1	42565
7	12	3	6	3	90065
2	5	3	2	5	47516
3	5	2	5	8	92798
2	11	3	5	2	45334
7	12	4	3	4	106704
7	10	3	7	1	88747
4	16	4	6	5	146157
1	6	8	6	5	39209
3	6	4	4	7	50344
6	9	3	3	3	116312
2	4	6	3	7	52750
4	9	3	1	3	70848
4	8	1	4	7	87446
4	18	2	7	5	150296
2	10	5	5	2	43405
4	11	3	3	4	66701
3	5	7	3	6	68149
3	11	4	2	7	68109
6	6	7	4	5	91151

Continued on next page

Table A.1 – continued from previous page

Angle Thk	Angle Ht	Base Thk	Bracket Thk	Beam Thk	Maximum RF
5	8	6	6	5	91151
3	6	2	6	2	91151
4	17	2	5	2	91151
4	1	5	3	5	91151
7	5	4	5	4	125243
4	10	3	5	4	61586
6	4	4	3	6	96978
7	3	3	2	2	133947
2	2	8	8	8	133947
3	9	6	7	2	46343
4	3	3	5	7	46343
1	1	7	8	6	46343
2	14	1	4	1	46471
2	2	8	8	8	48918
5	10	2	4	7	112357

3. Generations

Angle Thk	Angle Ht	Base Thk	Bracket Thk	Beam Thk	Maximum RF
1	5	1	1	6	32332
1	9	7	3	2	32385
2	11	7	7	5	32385
1	8	3	1	3	28846
2	10	2	3	3	51751
4	5	5	3	6	83029
4	11	2	2	4	72927
3	6	7	6	6	53390
2	4	2	4	2	50988
1	9	4	1	3	37046
2	9	4	2	2	37046
3	4	5	3	5	37046
2	11	2	4	2	42810
7	15	2	3	1	114020
2	14	4	7	2	61073
3	13	6	5	5	91778

Continued on next page

Table A.1 – continued from previous page

Angle Thk	Angle Ht	Base Thk	Bracket Thk	Beam Thk	Maximum RF
5	4	6	4	6	83242
3	2	7	5	2	46158
1	3	7	3	8	46158
2	10	7	7	2	40835
1	9	2	5	2	40835
2	12	8	4	1	47749
2	9	3	5	2	47749
2	10	2	5	2	42236
6	12	3	6	2	104088
2	5	7	6	6	52235
4	11	3	4	1	64126
4	7	7	1	5	74052
1	6	5	4	6	38165
4	10	2	3	3	38165
2	8	7	5	4	38165
6	2	3	5	7	87746
1	10	4	6	1	29692
1	19	2	1	1	42064
7	11	2	7	1	81220
1	18	5	7	2	40621
6	14	6	2	7	40621
4	2	3	5	8	69367
4	9	3	1	3	70848
3	17	2	5	1	63097
		4. Generations			
Angle Thk	Angle Ht	Base Thk	Bracket Thk	Beam Thk	Maximum RF
1	8	3	1	3	28846
1	10	4	6	1	29692
1	12	2	3	3	33436
2	8	5	5	2	44915
1	10	5	3	5	45800
1	10	3	2	3	45800
1	9	2	5	2	35338

Continued on next page

Table A.1 – continued from previous page

Angle Thk	Angle Ht	Base Thk	Bracket Thk	Beam Thk	Maximum RF
3	13	3	5	2	56422
8	9	4	7	1	125117
1	4	8	4	8	125117
1	9	3	5	3	28990
1	16	7	5	5	60530
1	6	1	2	3	60530
7	6	4	5	6	84674
6	10	6	4	4	95272
3	19	1	4	2	81367
2	9	6	4	5	48175
5	10	7	5	3	48175
4	12	3	4	4	48175
3	13	4	5	7	48175
5	2	6	3	2	48175
2	11	8	6	4	48175
1	15	2	8	1	48175
1	16	4	5	5	60659
3	12	5	6	5	74128
1	9	6	3	7	45602
2	8	2	4	2	46210
6	8	4	5	3	93239
1	7	6	4	5	33133
1	6	8	5	5	33133
6	1	4	6	6	103232
7	14	1	7	2	103232
1	10	1	4	3	40402
1	18	6	8	2	40402
1	8	2	1	3	40402
1	9	3	1	4	35598
3	1	8	2	7	71707
1	9	2	5	2	71707
3	3	4	2	6	71293
1	9	4	6	1	30877

Continued on next page

Table A.1 – continued from previous page

Angle Thk	Angle Ht	Base Thk	Bracket Thk	Beam Thk	Maximum RF
5. Generations					
Angle Thk	Angle Ht	Base Thk	Bracket Thk	Beam Thk	Maximum RF
1	8	3	1	3	28846
1	9	3	5	3	28846
1	11	3	2	3	35090
3	13	5	5	2	35090
3	9	4	4	8	60178
2	2	7	5	2	37510
1	10	3	2	3	38906
1	6	2	5	3	32569
1	10	4	1	3	32569
5	9	5	5	5	87086
1	5	7	5	5	38806
1	8	1	7	4	30957
4	6	3	7	4	30957
1	11	4	2	3	30957
2	16	7	5	7	124117
1	18	6	8	2	124117
2	8	3	3	4	124117
3	12	4	5	2	52170
4	10	3	5	4	52170
1	3	6	5	1	35295
1	10	2	5	2	35295
1	8	3	3	5	27116
2	5	4	3	4	50042
1	18	6	2	5	62130
2	16	4	6	3	54064
5	13	2	3	1	54064
1	10	3	2	3	54064
1	11	2	5	3	39794
1	10	2	5	2	39794
3	12	5	5	2	39794
1	11	3	4	4	39845

Continued on next page

Table A.1 – continued from previous page

Angle Thk	Angle Ht	Base Thk	Bracket Thk	Beam Thk	Maximum RF
1	7	1	6	7	64184
1	6	6	5	6	39459
2	10	5	5	5	39459
1	11	1	2	3	37433
1	8	3	1	2	32840
1	7	4	6	1	29100
1	13	2	1	2	37989
4	11	3	3	5	37989
1	8	4	1	4	37012

6. Generations

Angle Thk	Angle Ht	Base Thk	Bracket Thk	Beam Thk	Maximum RF
1	8	3	3	5	27116
1	8	3	1	3	28846
1	5	1	6	7	28846
1	12	2	2	2	28846
1	7	3	3	3	28846
1	7	4	5	1	22116
2	11	5	5	1	47133
1	1	8	5	4	41976
1	6	8	4	6	36523
1	12	4	3	3	32106
4	12	5	4	3	78704
4	11	2	3	3	72045
2	5	4	5	4	44736
1	8	4	1	3	32805
2	10	3	7	4	32805
1	8	3	2	5	38877
1	10	2	5	2	24117
1	6	3	6	7	47039
1	6	4	2	4	39098
4	11	3	5	7	39098
1	10	4	2	3	39173
1	13	4	5	1	39173

Continued on next page

Table A.1 – continued from previous page

Angle Thk	Angle Ht	Base Thk	Bracket Thk	Beam Thk	Maximum RF
1	8	2	8	5	30291
2	15	4	5	5	81331
1	10	7	1	3	81331
1	14	2	6	2	81331
1	10	4	7	3	35004
1	11	4	6	1	35004
1	8	4	2	3	39374
1	10	2	3	4	34567
1	6	4	5	2	34990
1	13	7	5	2	34990
1	7	2	4	5	34990
1	14	4	1	2	27012
2	4	2	7	2	39834
4	5	2	8	4	69772
1	12	4	2	4	69772
1	14	2	2	2	40753
1	7	3	4	6	40753
5	12	2	4	5	79279

7. Generations

Angle Thk	Angle Ht	Base Thk	Bracket Thk	Beam Thk	Maximum RF
1	7	4	5	1	22116
1	10	2	5	2	24117
3	9	2	5	3	52934
1	11	1	5	2	32885
1	8	3	2	4	35232
1	7	7	6	2	35232
5	7	4	4	4	35232
2	4	2	1	2	35232
1	6	3	5	4	35232
1	4	3	1	3	35232
1	9	2	7	4	32118
1	12	4	4	4	40872
1	12	2	6	2	36071

Continued on next page

Table A.1 – continued from previous page

Angle Thk	Angle Ht	Base Thk	Bracket Thk	Beam Thk	Maximum RF
1	16	3	3	3	45301
1	13	4	4	4	45301
1	10	4	7	3	35004
2	11	4	7	3	46282
1	8	4	6	2	46282
8	6	5	6	3	92518
1	10	4	4	3	33516
4	18	3	7	3	33516
7	8	5	5	5	105482
3	3	4	5	5	63384
1	8	3	2	5	38877
1	11	2	4	6	39895
1	12	6	3	3	32575
1	8	7	5	5	41878
1	7	4	3	2	27168
1	8	4	8	3	27168
1	9	2	2	2	27168
1	8	5	1	3	34019
2	11	2	4	2	42810
1	6	2	1	1	28024
1	5	1	5	8	102743
1	13	3	2	3	36721
1	4	1	7	7	39613
1	4	2	6	8	67405
1	9	8	4	5	35040
1	6	5	1	5	35040
1	8	4	1	2	33522
8. Generations					
Angle Thk	Angle Ht	Base Thk	Bracket Thk	Beam Thk	Maximum RF
1	7	4	5	1	22116
1	10	2	5	2	24117
1	10	3	2	3	38906
1	9	4	3	4	38906

Continued on next page

Table A.1 – continued from previous page

Angle Thk	Angle Ht	Base Thk	Bracket Thk	Beam Thk	Maximum RF
1	8	4	8	3	34738
1	12	8	3	2	36510
1	8	4	3	4	36510
1	11	4	5	4	36578
1	3	3	3	3	32891
1	11	6	3	3	33784
1	11	3	5	4	43646
1	5	4	2	1	43646
1	7	5	3	8	59215
1	7	2	5	7	38064
1	14	7	3	2	38064
1	7	6	2	3	43422
1	7	2	3	2	26426
6	12	3	3	3	86416
1	13	2	3	1	32026
1	11	3	3	3	28936
1	6	4	5	1	28936
1	12	2	7	5	62804
1	8	3	2	5	38877
1	6	3	1	4	40897
1	16	1	3	2	45622
1	13	2	8	3	46200
1	10	1	4	2	32124
6	12	3	7	1	92827
1	8	1	4	7	85517
1	9	7	8	5	40724
1	6	4	1	2	35858
1	9	6	4	4	32179
1	14	2	1	7	44282
1	11	2	6	2	44282
3	19	3	8	2	44282
1	10	2	1	1	31949
1	3	7	6	6	33492

Continued on next page

Table A.1 – continued from previous page

Angle Thk	Angle Ht	Base Thk	Bracket Thk	Beam Thk	Maximum RF
1	8	4	2	2	36382
1	4	2	6	8	67405
3	12	2	5	6	73194
9. Generations					
Angle Thk	Angle Ht	Base Thk	Bracket Thk	Beam Thk	Maximum RF
1	7	4	5	1	22116
1	10	2	5	2	24117
3	8	4	2	5	65399
1	8	5	2	2	31024
1	9	2	1	1	26543
1	12	1	6	1	30768
1	8	7	3	1	32699
1	6	3	4	2	32699
1	9	5	8	4	36840
1	7	4	2	3	36840
1	7	5	2	7	52600
1	4	8	3	2	28728
1	5	6	4	3	32267
1	8	3	6	1	28620
1	10	1	4	3	28620
1	9	3	7	2	32381
4	12	2	3	5	91191
1	10	3	5	4	91191
1	9	7	3	4	91191
1	7	3	3	2	29485
1	8	5	3	3	30972
1	11	4	3	2	30972
1	12	3	6	2	37392
1	13	3	4	2	37392
1	6	4	1	4	46430
1	11	7	4	2	38442
1	8	4	2	2	36382
1	10	1	3	2	36093

Continued on next page

Table A.1 – continued from previous page

Angle Thk	Angle Ht	Base Thk	Bracket Thk	Beam Thk	Maximum RF
1	8	3	4	2	36093
1	10	5	5	4	36723
1	4	3	2	2	28494
1	8	2	5	2	28494
1	10	3	2	2	29352
1	1	2	2	2	27018
1	8	8	8	5	35625
1	10	4	5	3	30399
1	17	3	2	1	30399
1	4	1	6	8	77401
1	17	1	3	3	77401
1	11	8	2	2	33687
10. Generations					
Angle Thk	Angle Ht	Base Thk	Bracket Thk	Beam Thk	Maximum RF
1	7	4	5	1	22116
1	10	2	5	2	22116
1	5	4	5	2	27979
1	7	5	1	2	30362
1	11	1	6	8	30362
1	5	5	2	2	21248
1	9	3	2	1	24219
1	14	1	6	1	39296
1	4	3	4	6	39296
1	6	3	4	4	37274
1	9	2	5	2	35338
1	7	4	3	1	27498
1	14	5	5	1	38304
1	6	7	2	2	38304
1	4	6	2	2	38304
1	10	2	5	2	24117
1	8	3	4	2	26968
1	9	4	5	5	37605
1	6	3	2	2	28687

Continued on next page

Table A.1 – continued from previous page

Angle Thk	Angle Ht	Base Thk	Bracket Thk	Beam Thk	Maximum RF
1	13	7	5	1	31942
1	7	5	4	2	31942
1	8	7	5	3	32061
1	8	7	3	1	32699
1	6	3	4	3	27688
1	3	6	6	1	31038
1	6	2	3	3	37415
1	8	2	1	1	24921
1	11	3	7	2	32945
1	6	2	2	2	32945
1	7	3	6	2	35654
1	8	4	6	3	33736
1	6	4	2	2	38066
1	9	6	1	2	31074
1	7	8	8	5	31074
1	2	8	2	2	31074
1	6	5	5	1	31074
1	5	2	5	2	31074
1	11	1	6	1	31074
1	1	2	1	2	31074
1	7	3	5	3	24097

A.2 Second Part Optimization Result

At this part, material is added as sixth variable. Material variable is defined at sixth column. The reaction force of this variables are given at last column. Part 2 Optimization Inputs and Results For Thicknesses [1 2 3 4 5 6 7 8] = [0.60 0.81 1.00 1.27 1.42 1.60 1.80 2.00] For Height [1 2 3 4 5 6 7 8 9 10 11 12 13 14 15 16 17 18 19] = [100 105 110 ... 185 190] For Material [1 2 3] = [Aluminum Titanium Magnesium]

Table A.2: Second Part Optimization Results

Initial Points						
Angle Thk	Angle Ht	Base Thk	Bracket Thk	Beam Thk	Material	Maximum RF
2	11	1	4	5	2	74615
4	3	3	5	6	2	87744
7	4	2	6	3	2	117690
8	6	7	1	5	1	104261
3	17	5	7	8	2	104261
7	5	7	6	4	2	118567
8	15	3	5	5	2	241913
4	5	3	5	2	3	49093
7	18	3	4	4	3	118734
2	7	1	3	5	1	52240
3	5	7	5	6	2	78896
8	6	5	5	3	3	78896
7	12	4	6	4	2	153474
7	10	3	6	8	1	146031
6	7	6	5	1	2	179363
1	16	5	3	7	2	145736
6	11	3	7	7	3	106383
7	11	4	5	6	2	143440
5	18	4	4	1	2	206018
7	7	2	8	2	2	88403
6	14	3	7	3	3	86013
4	14	2	4	6	2	142262
5	8	3	6	2	2	113924
2	11	3	6	6	3	50193
6	3	4	3	2	2	130973
1	1	1	3	5	1	21311
2	11	8	5	5	2	88441
1	15	8	2	7	3	49135
2	17	4	7	7	2	192131
6	3	5	2	7	2	106041
5	11	4	2	8	1	104694
4	10	7	2	3	1	78794

Continued on next page

Table A.2 – continued from previous page

Angle Thk	Angle Ht	Base Thk	Bracket Thk	Beam Thk	Material	Maximum RF
7	1	4	2	6	1	124074
2	7	2	5	2	1	38190
5	4	6	4	1	3	65482
4	15	4	8	7	3	130982
7	6	2	4	5	2	87615
7	10	4	2	4	2	169640
3	3	1	7	7	1	55047
5	12	2	8	6	2	190568
5	6	7	5	6	3	53951
6	12	8	1	7	3	76153
6	14	6	3	6	2	148997
6	15	2	4	6	3	88217
3	10	3	6	2	1	51134
6	2	4	2	3	3	81551
5	6	6	5	7	2	77694
2	17	1	5	1	3	39728
1	4	2	2	5	2	69013
4	15	3	2	2	2	138974
8	11	5	3	8	1	89546
3	18	6	4	6	1	135701
6	3	6	3	5	3	83475
3	9	5	5	4	1	53177
6	2	5	1	1	1	106089
2	19	3	3	6	3	105480
4	1	6	6	2	2	117980
6	14	3	2	2	3	81470
7	15	5	8	5	1	174775
7	16	2	7	1	1	129973
1	1	1	3	5	1	21311
2	7	2	5	2	1	38190
2	17	1	5	1	3	39728
3	4	1	3	5	1	58502
6	12	5	4	5	3	87950

Continued on next page

Table A.2 – continued from previous page

Angle Thk	Angle Ht	Base Thk	Bracket Thk	Beam Thk	Material	Maximum RF
5	14	2	5	6	3	111846
6	11	5	4	7	3	78816
1	14	7	3	4	1	54742
4	6	3	6	2	2	101808
3	3	1	5	2	3	42562
3	11	3	6	4	2	96313
5	6	5	8	7	2	93361
4	6	6	5	2	3	58956
6	1	5	5	5	2	102320
3	4	4	7	5	3	48438
5	6	5	5	5	2	78585
1	8	5	8	2	1	35671
5	6	4	5	3	1	74790
1	1	1	3	5	1	21311
2	7	2	2	5	1	46226
1. Generation						
Angle Thk	Angle Ht	Base Thk	Bracket Thk	Beam Thk	Material	Maximum RF
6	11	8	2	1	1	100659
2	7	1	6	5	1	45549
1	14	2	6	6	3	81706
7	9	1	5	2	1	98592
5	2	4	2	7	3	78089
5	9	5	2	3	3	78034
5	14	3	6	8	2	189377
2	17	1	6	5	3	92897
1	15	4	6	4	2	102240
4	19	6	7	2	3	86426
3	14	4	3	3	2	109541
3	10	3	6	2	1	51134
4	7	3	7	2	2	98755
5	16	1	5	2	3	82942
4	2	2	6	7	2	73757
5	6	6	5	5	2	79849

Continued on next page

Table A.2 – continued from previous page

Angle Thk	Angle Ht	Base Thk	Bracket Thk	Beam Thk	Material	Maximum RF
3	4	3	2	6	3	45982
4	4	1	4	6	1	75974
4	2	3	4	7	2	69878
6	7	4	2	8	2	93604
3	7	5	5	4	3	45219
2	11	3	7	4	2	76671
1	6	2	4	4	1	44417
3	6	3	6	5	1	57159
6	8	3	2	3	1	103411
2	7	1	6	2	1	43459
1	6	5	7	2	2	63815
1	7	1	3	5	1	45662
4	2	5	8	8	3	45905
8	1	7	8	2	1	115331
6	11	8	1	7	3	65831
2	15	7	8	8	3	91056
8	5	7	1	6	1	138220
1	19	2	8	8	2	150509
7	3	6	2	6	3	107571
2	11	2	5	6	3	60936
2	10	3	6	1	1	44126
5	7	7	5	8	3	72137
6	15	3	2	2	3	76107
2	17	5	8	8	2	203618
1	1	1	3	5	1	21311
1	1	1	3	5	1	21311
1	8	5	8	2	1	35671
3	3	3	2	7	2	95429
5	8	1	4	2	2	100626
4	16	5	2	4	3	64272
6	14	8	4	2	1	90394
4	9	4	3	8	2	88737
1	14	2	5	8	3	125538

Continued on next page

Table A.2 – continued from previous page

Angle Thk	Angle Ht	Base Thk	Bracket Thk	Beam Thk	Material	Maximum RF
5	11	5	2	3	3	66451
2	8	6	4	1	3	30423
4	3	2	5	2	2	123695
5	16	3	2	2	2	128658
6	6	3	4	5	2	96095
1	8	1	5	7	3	71948
2	19	2	5	4	3	76703
3	13	8	5	3	1	68142
2	15	4	6	1	2	117705
5	14	2	7	6	2	204895
2	15	1	6	5	3	69825
6	15	7	5	2	3	96728
5	15	4	6	8	1	176650
4	7	6	6	1	1	66733
1	9	4	6	2	2	45968
3	15	5	3	5	2	121729
2	19	7	3	6	3	103183
5	16	5	5	3	2	214465
4	12	6	5	5	2	123015
3	8	3	6	5	2	71670
4	7	5	4	2	3	55063
4	2	5	3	8	3	54561
1	8	4	2	7	2	55863
3	1	5	2	6	2	94773
6	17	6	3	2	3	86364
3	2	1	6	2	1	50821
4	7	3	4	6	2	69589
5	6	6	4	8	2	89167
1	10	6	6	4	1	41721
2	14	3	5	5	3	82596
8	10	4	6	5	1	101447
2. Generation						
Angle Thk	Angle Ht	Base Thk	Bracket Thk	Beam Thk	Material	Maximum RF

Continued on next page

Table A.2 – continued from previous page

Angle Thk	Angle Ht	Base Thk	Bracket Thk	Beam Thk	Material	Maximum RF
6	9	4	6	2	1	83176
4	10	6	2	5	3	59753
8	6	3	4	6	1	86437
1	7	3	3	4	2	65103
1	12	1	5	4	1	43209
2	18	5	6	8	2	184059
3	2	6	7	3	2	93570
5	7	5	2	5	1	89669
2	15	7	8	8	3	91056
1	12	1	4	6	3	60208
6	5	4	6	3	1	98055
3	3	3	2	7	3	55050
2	14	2	7	3	2	103738
3	4	1	5	6	1	60615
1	10	4	7	3	1	35004
1	1	1	1	2	1	27309
7	3	6	2	3	3	96115
3	17	1	5	1	3	49336
1	19	2	8	8	2	150509
3	10	4	4	4	1	58477
1	1	1	3	5	1	21311
1	1	1	3	5	1	21311
1	1	1	1	2	1	27309
4	4	1	3	4	1	77969
4	3	1	3	5	2	114786
1	11	4	4	2	3	27691
3	5	1	5	2	2	88364
3	2	7	3	5	2	92403
3	17	1	4	3	1	96758
1	1	3	1	4	1	35307
2	15	7	4	4	1	86407
3	12	5	4	3	2	85918
6	2	6	4	3	3	73711

Continued on next page

Table A.2 – continued from previous page

Angle Thk	Angle Ht	Base Thk	Bracket Thk	Beam Thk	Material	Maximum RF
1	11	5	4	3	1	35753
3	17	5	4	4	1	105222
4	8	4	2	4	3	61465
1	10	6	4	2	1	36766
2	16	4	5	2	1	48653
3	4	3	3	5	2	95749
5	10	8	6	2	2	106087
4	2	2	6	3	1	59640
4	4	1	6	2	2	102343
2	2	4	5	5	2	73986
5	11	2	4	2	1	81919
3	10	4	3	2	2	92949
3	4	3	2	7	3	44994
2	3	4	6	2	1	38454
1	17	3	5	2	3	33147
3	7	6	4	5	3	46577
2	2	6	4	7	1	52177
2	15	3	8	3	1	68131
2	10	3	6	3	2	68695
4	13	4	4	1	2	149221
5	10	5	7	4	1	77303
1	11	4	8	5	1	43272
7	13	6	4	3	1	98542
1	1	1	2	5	1	26501
7	5	6	6	7	1	72830
3	16	2	4	1	3	47119
4	7	6	7	2	1	69434
4	7	7	6	1	2	136763
2	11	2	5	2	1	47563
4	3	2	2	4	2	127848
2	10	5	5	4	2	80325
5	7	5	5	7	3	70365
5	9	5	5	2	3	65583

Continued on next page

Table A.2 – continued from previous page

Angle Thk	Angle Ht	Base Thk	Bracket Thk	Beam Thk	Material	Maximum RF
4	10	3	7	5	2	120651
6	3	3	5	2	3	80460
1	1	1	3	5	1	21311
2	10	3	4	4	1	45911
1	1	1	1	2	1	27309
2	1	7	8	3	2	69388
2	19	1	6	3	3	61813
1	14	4	5	5	3	53150
6	7	8	6	2	1	99255
1	16	4	6	1	1	38950
2	7	3	6	6	2	68743
1	6	3	3	4	2	53862
1	1	1	2	4	1	32167
4	10	5	1	5	3	63470
			3. Generation			
Angle Thk	Angle Ht	Base Thk	Bracket Thk	Beam Thk	Material	Maximum RF
1	1	1	3	5	1	21311
1	1	1	3	5	1	21311
1	1	1	3	5	1	21311
2	5	1	3	3	2	76063
2	10	4	4	3	1	39533
1	9	2	5	2	1	35338
7	16	1	8	2	1	138353
6	6	5	6	6	1	72098
3	11	7	4	3	2	105627
1	16	4	7	5	1	61154
2	10	4	5	3	1	36198
2	1	5	5	1	2	60755
1	8	3	2	7	1	45230
1	19	3	4	6	2	132387
1	16	2	4	3	1	46672
8	1	5	7	2	2	138195
5	6	2	3	4	2	106692

Continued on next page

Table A.2 – continued from previous page

Angle Thk	Angle Ht	Base Thk	Bracket Thk	Beam Thk	Material	Maximum RF
2	11	4	5	2	1	44030
3	10	5	2	2	2	86343
6	11	2	4	5	1	95881
7	8	4	4	2	3	85699
1	1	1	3	5	1	21311
6	10	7	5	7	1	99394
2	2	5	6	8	1	50382
5	11	8	3	2	1	82116
3	12	5	3	4	1	52933
2	2	3	3	4	1	45717
2	5	3	7	3	2	71841
3	9	2	4	3	2	94351
1	13	3	4	5	3	56292
6	18	4	5	2	2	247435
3	1	4	6	5	3	48914
3	11	4	6	3	2	95228
2	10	7	3	4	2	81124
1	12	7	3	4	1	43646
2	10	4	4	3	3	41787
2	1	4	7	2	1	48045
1	8	6	4	5	2	56453
1	3	4	8	3	3	29983
2	17	3	6	3	2	106500
2	2	2	4	2	2	67690
1	14	2	5	5	2	109196
7	8	7	3	2	2	165494
4	7	2	4	3	3	56214
3	11	1	4	4	2	99165
3	2	4	2	7	3	50431
1	1	1	5	2	1	29111
1	15	3	2	3	1	37385
2	18	4	4	2	1	54269
6	2	5	3	4	3	83742

Continued on next page

Table A.2 – continued from previous page

Angle Thk	Angle Ht	Base Thk	Bracket Thk	Beam Thk	Material	Maximum RF
1	10	1	4	1	1	34271
1	7	3	3	4	2	65103
1	18	8	8	2	1	36934
3	19	1	7	4	3	94492
6	1	7	2	3	3	86107
3	15	2	4	1	3	45215
1	1	1	1	2	1	27309
1	6	7	6	2	1	25112
1	1	1	3	5	1	21311
1	1	1	2	4	1	32167
1	1	1	3	5	1	21311
1	1	1	3	5	1	21311
1	1	1	3	5	1	21311
2	13	5	4	5	1	80154
1	4	6	4	7	3	42610
4	17	4	8	2	2	190173
2	16	4	7	2	1	50111
2	11	5	2	5	1	55860
3	1	4	6	2	1	52780
3	8	8	2	3	2	100281
1	3	1	5	6	1	27553
2	8	3	4	4	2	73435
2	8	4	5	2	1	36073
4	10	3	4	2	2	110071
2	6	4	4	7	3	44165
1	1	1	2	4	1	32167
3	16	6	5	2	1	61890
7	1	2	4	2	2	128730
1	9	1	2	5	1	29456
1	16	2	3	3	1	54183
4. Generation						
Angle Thk	Angle Ht	Base Thk	Bracket Thk	Beam Thk	Material	Maximum RF
2	1	4	7	2	2	80694

Continued on next page

Table A.2 – continued from previous page

Angle Thk	Angle Ht	Base Thk	Bracket Thk	Beam Thk	Material	Maximum RF
1	10	3	7	5	2	86301
2	1	4	2	5	1	57417
1	10	3	5	1	1	33256
4	1	5	6	5	2	84791
3	11	5	1	3	2	99568
1	6	6	4	4	2	59739
2	10	3	3	5	3	41450
1	2	4	1	3	2	52081
6	10	7	5	4	1	82811
3	7	2	5	1	2	78969
3	15	2	4	1	3	45215
2	18	5	6	2	1	49845
1	1	1	2	2	1	26839
2	14	2	5	5	2	119833
6	5	7	3	4	3	76470
3	7	2	4	3	3	46261
4	8	7	5	3	2	99273
2	17	5	5	6	2	184687
4	1	7	3	4	1	86795
3	7	2	4	3	2	85557
3	17	7	4	3	1	86947
2	18	2	6	1	2	73300
1	8	2	6	2	3	26781
4	2	3	6	1	1	59567
4	7	2	4	3	3	56214
1	16	1	4	5	1	79722
1	9	7	2	2	1	29991
2	1	4	4	5	3	35843
3	13	5	2	3	1	59365
1	1	1	3	5	1	21311
1	17	4	7	5	1	63640
1	16	3	2	2	1	42064
1	1	1	2	6	1	57615

Continued on next page

Table A.2 – continued from previous page

Angle Thk	Angle Ht	Base Thk	Bracket Thk	Beam Thk	Material	Maximum RF
2	19	4	3	1	1	61424
1	1	1	2	5	1	26501
1	14	2	5	4	3	53555
2	16	1	3	1	3	34341
1	1	1	6	6	1	25512
1	11	1	4	1	1	31107
1	1	1	3	5	1	21311
1	1	1	3	5	1	21311
1	1	1	3	5	1	21311
3	14	1	3	5	2	107537
4	14	4	5	1	2	177499
1	7	2	5	1	2	58380
2	1	8	2	5	1	58477
5	10	2	6	5	1	85099
1	10	5	4	5	1	36759
3	11	2	2	5	1	59465
1	1	1	3	5	1	21311
1	4	7	2	2	1	27672
4	6	2	3	5	1	62328
2	16	3	3	1	3	33402
1	11	3	2	1	3	21159
2	12	1	4	2	3	33449
3	14	6	3	7	3	57683
2	5	4	6	2	1	45256
3	16	6	3	7	2	180308
3	9	5	3	4	2	107352
1	3	3	2	1	1	33941
2	16	3	3	2	1	53101
1	16	4	4	1	2	49837
2	4	7	2	5	2	76296
2	7	6	4	4	2	73876
2	5	4	4	2	2	71687
2	1	4	3	5	1	48482

Continued on next page

Table A.2 – continued from previous page

Angle Thk	Angle Ht	Base Thk	Bracket Thk	Beam Thk	Material	Maximum RF
5	1	2	6	5	2	116910
1	1	1	3	5	1	21311
1	9	2	5	2	1	21311
2	14	4	4	4	3	61817
1	1	1	2	6	1	57615
2	8	4	3	2	3	32497
1	5	8	3	6	2	64164
3	7	4	5	6	1	51006
1	8	3	7	5	3	24854
8	11	5	4	4	1	89917
6	4	1	5	4	3	81943
1	2	4	5	2	1	30828
1	17	7	3	1	1	36049
			5. Generation			
Angle Thk	Angle Ht	Base Thk	Bracket Thk	Beam Thk	Material	Maximum RF
3	6	5	5	1	2	36049
2	8	5	4	3	3	32919
2	1	3	2	4	2	83514
1	11	2	4	2	1	31092
1	9	3	5	2	3	26694
1	7	4	5	2	1	32146
2	19	5	3	5	1	95324
1	1	1	3	5	1	21311
3	13	2	3	1	2	84412
2	15	2	4	1	3	35002
3	9	8	6	3	1	51029
1	1	1	7	6	1	31038
1	9	3	4	5	3	27054
1	1	1	1	7	1	33537
1	11	5	2	5	1	39945
2	19	1	8	8	1	149295
2	12	6	1	4	1	52281
1	1	1	8	8	1	46740

Continued on next page

Table A.2 – continued from previous page

Angle Thk	Angle Ht	Base Thk	Bracket Thk	Beam Thk	Material	Maximum RF
1	11	3	6	1	1	27602
2	1	7	7	2	3	27701
1	11	3	2	1	3	21159
1	1	1	3	5	1	21311
1	1	1	3	5	1	21311
4	14	1	3	3	1	73901
2	15	2	4	2	2	92060
4	9	7	2	4	1	78518
1	10	2	7	3	1	32535
2	1	7	7	2	3	27701
1	9	2	5	2	2	54462
1	1	1	2	5	1	26501
2	11	1	4	5	2	74615
4	3	3	5	6	2	87744
7	4	2	6	3	2	117690
8	6	7	1	5	1	104261
3	17	5	7	8	2	104261
7	5	7	6	4	2	118567
8	15	3	5	5	2	241913
4	5	3	5	2	3	49093
7	18	3	4	4	3	118734
2	7	1	3	5	1	52240
3	5	7	5	6	2	78896
8	6	5	5	3	3	78896
7	12	4	6	4	2	153474
7	10	3	6	8	1	146031
6	7	6	5	1	2	179363
1	16	5	3	7	2	145736
6	11	3	7	7	3	106383
7	11	4	5	6	2	143440
5	18	4	4	1	2	206018
7	7	2	8	2	2	206018
6	14	3	7	3	3	86013

Continued on next page

Table A.2 – continued from previous page

Angle Thk	Angle Ht	Base Thk	Bracket Thk	Beam Thk	Material	Maximum RF
4	14	2	4	6	2	142262
5	8	3	6	2	2	113924
2	11	3	6	6	3	50193
6	3	4	3	2	2	130973
1	1	1	3	5	1	21311
2	11	8	5	5	2	88441
1	15	8	2	7	3	49135
2	17	4	7	7	2	192131
6	3	5	2	7	2	106041
5	11	4	2	8	1	104694
4	10	7	2	3	1	78794
7	1	4	2	6	1	124074
2	7	2	5	2	1	38190
5	4	6	4	1	3	65482
4	15	4	8	7	3	130982
7	6	2	4	5	2	87615
7	10	4	2	4	2	169640
3	3	1	7	7	1	55047
5	12	2	8	6	2	190568
5	6	7	5	6	3	53951
6	12	8	1	7	3	76153
6	14	6	3	6	2	148997
6	15	2	4	6	3	88217
3	10	3	6	2	1	51134
6	2	4	2	3	3	81551
5	6	6	5	7	2	77694
2	17	1	5	1	3	39728
1	4	2	2	5	2	69013
4	15	3	2	2	2	138974
6. Generation						
Angle Thk	Angle Ht	Base Thk	Bracket Thk	Beam Thk	Material	Maximum RF
8	11	5	3	8	1	89546
3	18	6	4	6	1	135701

Continued on next page

Table A.2 – continued from previous page

Angle Thk	Angle Ht	Base Thk	Bracket Thk	Beam Thk	Material	Maximum RF
6	3	6	3	5	3	83475
3	9	5	5	4	1	53177
6	2	5	1	1	1	106089
2	19	3	3	6	3	105480
4	1	6	6	2	2	117980
6	14	3	2	2	3	81470
7	15	5	8	5	1	174775
7	16	2	7	1	1	129973
1	1	1	3	5	1	21311
2	7	2	5	2	1	38190
2	17	1	5	1	3	39728
3	4	1	3	5	1	58502
6	12	5	4	5	3	87950
5	14	2	5	6	3	111846
6	11	5	4	7	3	78816
1	14	7	3	4	1	54742
4	6	3	6	2	2	101808
3	3	1	5	2	3	42562
3	11	3	6	4	2	96313
5	6	5	8	7	2	93361
4	6	6	5	2	3	58956
6	1	5	5	5	2	102320
3	4	4	7	5	3	48438
5	6	5	5	5	2	78585
1	8	5	8	2	1	35671
5	6	4	5	3	1	74790
1	1	1	3	5	1	21311
2	4	1	2	4	1	49301
7	12	8	2	3	1	105078
2	3	2	7	2	1	48411
2	11	6	6	6	3	45843
3	9	3	2	2	1	56676
8	3	6	2	6	1	129847

Continued on next page

Table A.2 – continued from previous page

Angle Thk	Angle Ht	Base Thk	Bracket Thk	Beam Thk	Material	Maximum RF
2	5	5	5	3	1	44433
5	14	3	3	7	1	93777
2	17	1	4	1	2	88641
5	10	3	5	3	2	84858
4	3	4	8	2	2	118485
7	13	8	2	2	2	184139
3	10	3	6	2	1	51134
5	8	3	6	2	1	91932
5	12	5	2	2	3	75365
4	2	2	6	2	2	113787
4	5	6	5	6	2	86846
2	3	6	4	7	2	53833
3	5	1	3	6	2	95838
5	8	3	5	6	3	67911
6	12	4	5	8	1	142924
7	11	7	6	4	3	81491
4	11	3	4	6	3	59639
7	5	2	4	4	3	92293
3	12	3	6	2	1	52634
4	9	5	2	4	1	86678
2	7	2	4	5	1	51809
1	6	6	6	2	1	30867
5	5	1	3	5	1	92382
5	14	4	7	8	2	203042
8	6	8	5	3	3	203042
6	15	8	1	8	3	102418
7	4	7	7	6	3	73617
8	7	8	1	5	1	145004
2	18	8	2	8	2	135818
5	2	5	4	5	3	70975
2	12	4	6	7	3	62582
2	10	4	6	2	1	48838
5	6	5	5	7	2	82184

Continued on next page

Table A.2 – continued from previous page

Angle Thk	Angle Ht	Base Thk	Bracket Thk	Beam Thk	Material	Maximum RF
6	15	2	2	2	3	73145
2	16	5	6	8	2	213341
1	1	1	3	5	1	21311
1	1	1	3	5	1	21311
1	6	6	6	2	1	30867
2	11	5	4	7	2	108896
7	9	3	3	4	2	113995
5	4	7	4	3	1	84264
2	11	6	2	2	3	34906
4	11	2	6	4	3	62597
6	10	7	4	3	1	98914
6	6	6	7	3	1	79895
7. Generation						
Angle Thk	Angle Ht	Base Thk	Bracket Thk	Beam Thk	Material	Maximum RF
3	5	8	3	4	1	60299
3	3	7	5	2	3	46993
4	5	5	7	3	2	116004
4	5	6	8	3	1	73003
3	5	2	5	2	3	41158
2	12	4	6	8	1	103656
2	16	1	3	8	1	77780
4	10	2	6	2	1	62909
5	13	3	4	2	1	73369
2	18	3	3	2	2	97492
6	6	3	2	5	3	78722
7	3	2	3	4	3	102045
3	9	3	3	5	3	50905
1	2	1	2	5	1	38010
5	4	7	5	6	2	83549
3	6	1	3	3	1	63434
6	12	6	3	2	3	80729
1	11	4	2	7	1	57773
2	10	6	6	4	2	88170

Continued on next page

Table A.2 – continued from previous page

Angle Thk	Angle Ht	Base Thk	Bracket Thk	Beam Thk	Material	Maximum RF
4	9	3	6	2	2	107354
3	4	2	4	5	2	77027
6	5	4	5	3	1	100942
2	11	5	6	6	2	108435
3	4	1	3	5	1	58502
2	8	3	5	4	1	48355
1	13	3	2	4	3	40611
4	8	8	7	5	3	55757
5	4	3	5	6	2	80240
4	5	4	5	3	3	61358
2	8	4	5	6	2	65232
3	10	3	6	2	1	51134
3	6	3	4	3	1	54397
5	7	2	1	5	1	87771
1	11	3	4	2	1	30184
3	8	4	4	4	1	60153
4	11	3	4	6	3	59639
3	15	7	3	5	2	137753
5	17	1	4	5	1	136087
7	4	7	7	6	3	73617
2	10	6	5	6	3	55052
6	5	3	4	4	1	98347
1	10	6	6	6	3	42963
4	12	3	2	1	1	86019
2	2	1	2	8	3	79168
1	12	6	6	7	3	59005
1	1	1	4	5	1	22166
7	2	2	2	7	3	106033
2	15	1	5	1	3	39097
1	18	8	2	8	1	76701
3	12	3	6	1	1	56097
1	1	1	3	5	1	21311
1	1	1	3	5	1	21311

Continued on next page

Table A.2 – continued from previous page

Angle Thk	Angle Ht	Base Thk	Bracket Thk	Beam Thk	Material	Maximum RF
1	1	1	4	5	1	22166
2	4	1	6	8	1	77112
3	3	3	3	5	3	49826
3	4	3	2	4	1	58116
2	13	2	5	6	1	105248
2	11	6	6	5	2	96437
1	4	1	5	5	3	20326
5	3	4	5	7	2	81162
3	5	3	3	4	1	57728
4	10	4	7	4	1	73274
2	3	2	5	4	2	73691
5	11	5	5	7	2	156605
1	4	3	4	7	1	38793
5	18	7	4	3	1	126713
2	3	2	4	5	2	72909
3	6	7	7	1	1	48714
1	10	6	4	2	2	56071
1	12	5	3	1	3	23843
3	2	5	3	5	2	107011
2	9	6	4	4	3	35962
5	1	4	5	3	3	68151
2	2	4	6	7	3	27685
2	11	5	6	4	1	45149
1	11	4	6	4	2	71931
3	2	5	6	4	1	51195
3	5	6	2	3	3	50271
7	9	5	6	5	2	84414
5	3	5	4	2	1	89674
8. Generation						
Angle Thk	Angle Ht	Base Thk	Bracket Thk	Beam Thk	Material	Maximum RF
4	5	8	3	5	1	82505
2	11	6	1	2	3	34769
5	14	4	4	6	2	156027

Continued on next page

Table A.2 – continued from previous page

Angle Thk	Angle Ht	Base Thk	Bracket Thk	Beam Thk	Material	Maximum RF
2	11	6	2	2	3	34906
5	12	6	6	6	3	91638
2	6	6	4	5	1	42814
1	19	2	6	5	1	68461
1	14	1	4	5	1	81600
1	8	6	3	7	1	46097
3	4	3	6	3	1	51390
2	15	1	5	1	3	39097
4	5	2	5	1	2	93191
2	11	4	2	3	3	35711
4	14	5	7	2	2	190283
4	11	3	3	2	1	66713
3	14	4	4	3	2	118769
6	6	4	4	3	3	78712
5	12	6	3	4	1	92872
2	7	3	2	3	1	42301
2	7	3	5	6	1	52785
1	1	1	3	6	1	40097
1	10	6	1	2	3	28965
1	1	1	4	6	1	27605
1	14	4	2	3	3	27871
2	12	3	6	8	1	87747
3	6	4	4	3	3	50593
5	4	7	5	4	1	93024
1	11	3	4	1	1	26526
1	1	1	3	5	1	21311
4	5	2	4	3	1	73659
1	4	1	5	5	3	20326
1	1	1	3	5	1	21311
1	1	1	3	5	1	21311
3	2	2	8	5	1	52424
3	4	3	3	2	3	37491
2	1	1	5	4	2	75867

Continued on next page

Table A.2 – continued from previous page

Angle Thk	Angle Ht	Base Thk	Bracket Thk	Beam Thk	Material	Maximum RF
6	6	3	4	2	1	82521
5	3	1	5	5	2	117463
1	4	6	1	6	1	28236
2	12	1	5	3	3	31402
3	15	7	4	6	3	102643
5	3	3	6	7	3	64879
1	10	5	5	3	3	25580
1	1	1	4	7	1	60995
1	11	2	3	8	1	119921
3	9	4	6	4	3	40314
1	9	3	4	8	1	85730
5	5	1	4	5	1	91339
3	1	2	4	4	3	38453
1	2	6	3	5	2	70293
1	11	3	4	2	1	30184
2	9	2	2	5	3	40083
3	11	5	4	6	2	106702
2	17	2	6	4	2	144070
2	17	1	2	6	2	120390
2	4	3	3	6	3	37181
3	7	2	6	1	1	55095
1	19	5	7	3	3	44182
1	11	3	3	2	2	57700
3	5	5	4	6	2	98028
2	4	8	1	5	3	48201
2	11	7	3	2	2	63676
2	13	6	3	2	3	34493
2	5	5	3	6	2	74825
4	3	1	1	4	1	84916
7	11	6	5	1	3	78045
1	5	3	3	5	1	43511
6	4	3	4	4	2	149053
2	15	3	5	5	1	82327

Continued on next page

Table A.2 – continued from previous page

Angle Thk	Angle Ht	Base Thk	Bracket Thk	Beam Thk	Material	Maximum RF
5	7	3	4	3	1	88460
4	10	6	3	2	3	88460
1	10	5	6	3	1	29544
2	7	5	2	3	2	88122
4	2	5	4	3	3	51849
1	14	1	4	5	1	81600
2	3	2	7	7	3	36525
3	11	2	3	2	2	94737
3	7	5	3	3	3	44103
1	7	2	6	6	2	63134
3	1	5	6	3	1	62490
9. Generation						
Angle Thk	Angle Ht	Base Thk	Bracket Thk	Beam Thk	Material	Maximum RF
3	4	7	8	1	1	63227
4	5	2	4	1	1	66460
1	13	3	4	1	1	28727
1	4	1	4	6	3	35036
1	1	1	3	7	1	77222
1	1	1	4	5	1	22166
2	2	1	5	5	3	38974
1	5	8	1	1	3	23145
1	1	1	2	7	1	94449
1	1	1	4	7	1	60995
1	4	1	5	5	3	20326
1	1	1	3	5	1	21311
1	1	1	3	5	1	21311
1	12	4	6	8	2	123231
2	4	3	6	4	3	40362
1	10	5	6	3	1	29544
5	13	5	3	5	1	73309
2	2	3	5	5	3	31886
6	3	2	6	6	3	85087
1	15	3	3	2	2	67561

Continued on next page

Table A.2 – continued from previous page

Angle Thk	Angle Ht	Base Thk	Bracket Thk	Beam Thk	Material	Maximum RF
1	1	6	5	4	3	24582
3	7	2	7	4	3	46944
2	10	1	5	6	3	64715
1	4	3	5	6	2	64715
2	11	2	6	3	2	68265
1	10	8	1	3	3	30086
1	3	8	1	7	2	77956
3	12	6	4	4	2	77956
2	9	2	2	5	3	40083
1	1	2	4	3	2	65229
2	2	1	4	1	1	43027
2	4	2	7	3	2	67616
1	12	3	6	8	3	89650
1	11	3	6	2	3	26165
2	7	1	5	6	1	47006
1	4	2	3	5	1	41611
1	1	1	5	5	2	59642
1	19	4	3	3	1	59386
2	16	4	6	3	2	84170
6	6	4	4	3	2	102513
4	2	5	6	8	3	52746
2	3	4	5	4	1	49642
1	10	2	4	6	3	43223
1	12	6	3	7	3	52592
3	4	5	4	1	2	89552
1	11	4	7	8	3	82281
2	4	1	6	6	2	60813
1	4	6	1	6	1	28236
2	1	1	4	8	2	72402
1	1	1	3	5	1	21311
2	10	5	7	4	2	84800
1	16	2	2	5	1	69050
2	3	3	2	2	3	29169

Continued on next page

Table A.2 – continued from previous page

Angle Thk	Angle Ht	Base Thk	Bracket Thk	Beam Thk	Material	Maximum RF
6	4	5	5	3	3	76629
1	4	3	6	6	3	28031
1	5	5	2	3	3	19299
1	14	3	5	2	3	35479
2	2	2	3	5	1	43196
1	1	2	3	4	1	31111
3	1	5	7	3	1	59044
2	3	3	3	7	3	40872
1	8	6	1	7	1	37574
1	10	5	6	3	3	28232
1	2	7	1	7	3	27727
1	10	5	6	2	1	30109
1	19	5	7	4	3	47951
1	1	1	4	4	1	30194
1	3	8	1	6	3	24854
1	1	1	3	6	1	40097
2	14	6	3	1	3	34590
1	5	5	2	3	3	19299
1	4	1	5	5	3	20326
1	1	1	3	5	1	21311
1	3	6	5	5	2	21311
1	1	8	4	6	1	39455
5	8	4	6	2	3	65558
2	15	2	3	5	3	79813
6	13	5	7	2	3	74694
1	2	6	6	8	3	42117
1	15	3	6	3	3	39431
10. Generation						
Angle Thk	Angle Ht	Base Thk	Bracket Thk	Beam Thk	Material	Maximum RF
2	4	3	7	7	3	40448
5	4	2	4	3	3	69511
1	17	4	5	5	3	46308
1	7	7	3	7	3	40812

Continued on next page

Table A.2 – continued from previous page

Angle Thk	Angle Ht	Base Thk	Bracket Thk	Beam Thk	Material	Maximum RF
1	2	6	1	5	1	42820
2	10	4	3	1	1	40786
1	4	5	6	5	3	26977
1	2	3	2	3	2	81582
1	4	6	7	4	3	81582
1	1	4	2	3	3	23167
1	4	7	2	7	3	31759
1	5	2	5	5	3	22246
1	4	6	4	1	2	60342
1	7	2	2	3	3	24913
1	3	1	3	6	3	34509
1	5	6	7	6	2	34509
1	5	6	2	3	2	58174
1	3	2	3	6	3	24115
1	6	1	3	5	3	26388
1	7	7	5	1	2	26388
1	2	3	4	5	3	26388
1	3	4	7	2	3	24089
1	8	5	6	5	3	27179
1	10	5	8	7	3	51372
1	5	2	7	5	1	40380
1	10	3	7	5	3	36271
1	10	5	5	5	1	42205
7	18	6	3	7	3	146439
1	3	7	1	7	1	41785
1	12	7	3	4	1	43646
1	17	5	6	3	2	99007
1	4	1	1	6	1	37423
1	14	3	5	2	2	71618
1	2	2	3	3	1	30712
3	4	2	4	4	3	30712
2	11	4	7	6	3	45663
1	13	3	4	3	3	34437

Continued on next page

Table A.2 – continued from previous page

Angle Thk	Angle Ht	Base Thk	Bracket Thk	Beam Thk	Material	Maximum RF
2	10	2	4	5	3	34437
1	1	8	3	4	2	69722
1	4	6	3	3	3	32719
2	1	2	5	5	3	42369
1	1	1	4	6	1	27605
1	3	3	7	7	3	27605
1	5	3	4	8	3	59369
1	1	1	3	4	1	21239
1	1	3	6	5	3	29860
1	17	6	6	2	3	38222
1	11	2	6	2	3	26341
1	19	1	1	8	1	70337
1	2	8	1	7	3	31186
1	5	5	2	3	3	19299
1	4	1	5	5	3	19299
1	1	1	3	4	1	19299
1	12	6	6	4	3	35390
1	4	5	8	3	3	35390
1	5	1	4	3	3	35390
2	4	3	3	7	3	39782
1	18	4	6	7	2	39782
4	2	5	4	5	3	39782
1	11	3	6	6	3	40829
2	11	2	6	5	3	40829
1	1	3	2	3	3	20457
2	4	2	4	2	3	20457
1	15	6	6	5	3	47693
1	19	7	8	2	2	39797
1	6	7	4	5	3	32599
1	4	4	7	5	3	23379
1	4	5	1	7	1	23379
1	7	1	2	5	1	38080
1	2	2	2	7	1	45342

Continued on next page

Table A.2 – continued from previous page

Angle Thk	Angle Ht	Base Thk	Bracket Thk	Beam Thk	Material	Maximum RF
3	12	1	6	3	1	53887
1	8	8	6	1	3	21655
1	7	6	3	2	3	20076
1	5	2	3	5	3	24744
1	16	1	5	1	2	57140
1	6	2	4	2	3	27400
1	3	3	7	6	3	19942
1	3	7	2	6	3	27605
1	17	2	7	2	3	38475
1	5	5	2	3	3	19299